Cours 20-10-2014

Adult neurogenesis in non-mammalian vertebrates

Prisca Chapouton,[1] Ravi Jagasia,[2] and Laure Bally-Cuif[1]*
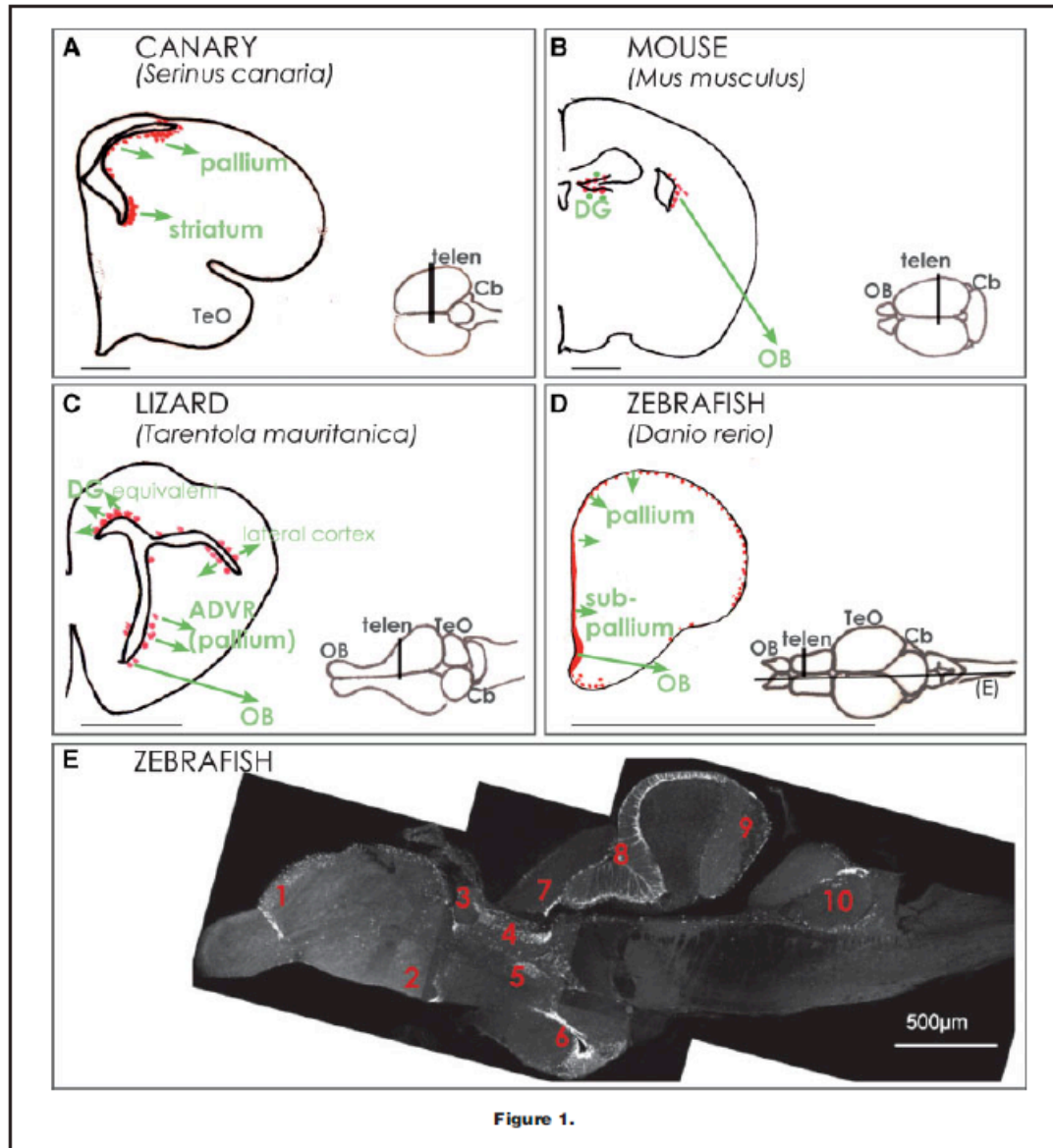

Figure 1.

Off the beaten track: new neurons in the adult human striatum
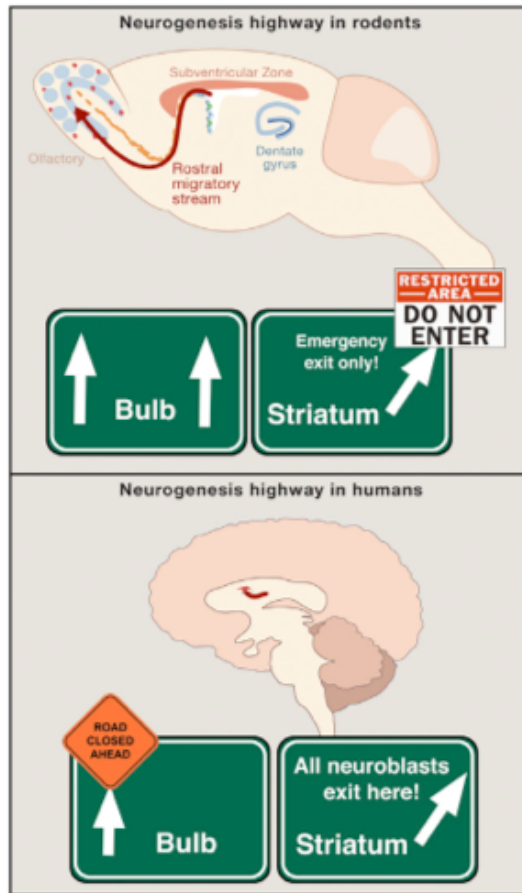
Kempermann G

Figure 1. Striatal Neurogenesis in Humans
Whereas neuroblasts from the adult subventricular zone (SVZ) in rodents migrate to the olfactory bulb to become interneurons, and enter the striatum only under pathological conditions such as ischemia (top), in humans hardly any adult neurogenesis can be found in the adult olfactory bulb, but it occurs to substantial degree in the striatum (Ernst et al., 2014).

Dynamics of hippocampal neurogenesis in adult humans

Spalding KL, Bergmann O, Alkass K, Bernard S, Salehpour M, Huttner HB, Boström E, Westerlund I, Vial C, Buchholz BA, Possnert G, Mash DC, Druid H, Frisén J

mature neurons in experimental animals are not readily applicable to humans. To be able to study cell turnover dynamics in humans, we have developed a strategy to retrospectively birth date cells (Spalding et al., 2005a). This strategy takes advantage of the elevated atmospheric ^{14}C levels caused by above-ground nuclear bomb testing in 1955–1963 during the Cold War (De Vries, 1958; Nydal and Lövseth, 1965). Since the Partial Nuclear Test Ban Treaty in 1963, atmospheric levels of ^{14}C have declined because of uptake by the biotope and diffusion from the atmosphere (Levin and Kromer, 2004; Levin et al., 2010). ^{14}C in the atmosphere reacts with oxygen to form CO_2, which is taken up by plants in photosynthesis. When we eat plants, or animals that live off plants, we take up ^{14}C, meaning that atmospheric ^{14}C levels are mirrored in the human body at all times (Harkness, 1972; Libby et al., 1964; Spalding et al., 2005b). When a cell goes through mitosis and duplicates its chromosomes, it integrates ^{14}C in the synthesized genomic DNA with a concentration corresponding to that in the atmosphere at the time, creating a date mark in the DNA (Spalding et al., 2005a). The cumulative nature of ^{14}C integration makes the method especially suited for establishing the kinetics of slowly turning over cell populations. The accuracy of individual datings is approximately ± 1.5 years (Spalding et al., 2005b), but higher accuracy is reached by integrating data from many independent measurements.
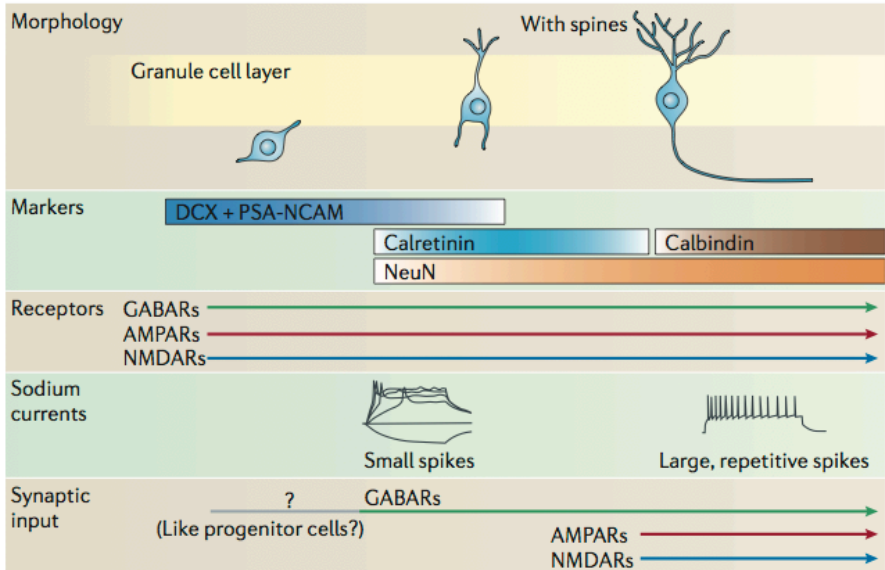
Adult neurogenesis and functional plasticity in neuronal circuits

Lledo P, Alonso M, Grubb M

Hippocampal granule cells

Approximate cell age (days): 2 · 14 · 28

Morphology — Granule cell layer — With spines

Markers: DCX + PSA-NCAM; Calretinin; Calbindin; NeuN

Receptors: GABARs; AMPARs; NMDARs

Sodium currents: Small spikes; Large, repetitive spikes

Synaptic input: ? GABARs (Like progenitor cells?); AMPARs; NMDARs

Olfactory bulb granule cells

Approximate cell age (days): 2 · 14 · 28

Morphology — External plexiform layer — Granule cell layer — With spines — Rostral migratory stream

Markers: DCX + PSA-NCAM; TUJ1 + TUC-4; NeuN

Receptors: GABARs; AMPARs; NMDARs

Sodium currents: No spikes; Spikes

Synaptic input: GABARs; AMPARs; NMDARs
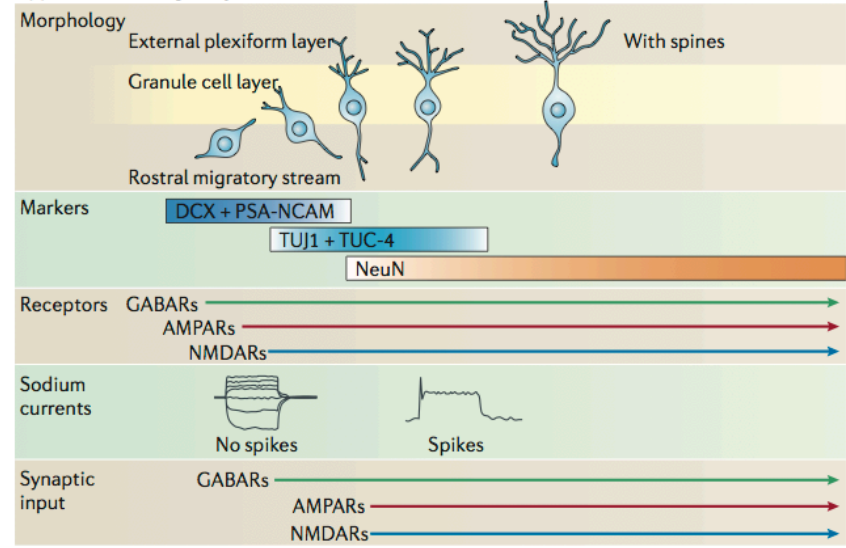
Olfactory bulb periglomerular cells

Approximate cell age (days): 2 · 14 · 28

Morphology — Glomerular layer — External plexiform layer — Granule cell layer — Rostral migratory stream

Markers: DCX + PSA-NCAM; TUJ1 + TUC-4; NeuN + GAD/Calbindin/Calretinin; TH

Receptors: GABARs; AMPARs; ?; NMDARs

Sodium currents: No spikes; Spikes

Synaptic input: GABARs; AMPARs; NMDARs

Neurogenesis in the striatum of the adult human brain
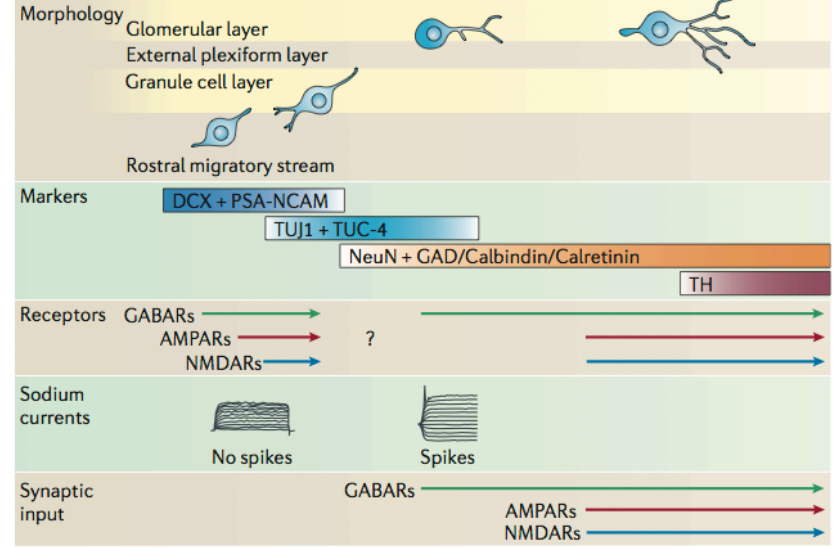
Ernst A, Alkass K, Bernard S, Salehpour M, Perl S, Tisdale J, Possnert G, Druid H, Frisén J
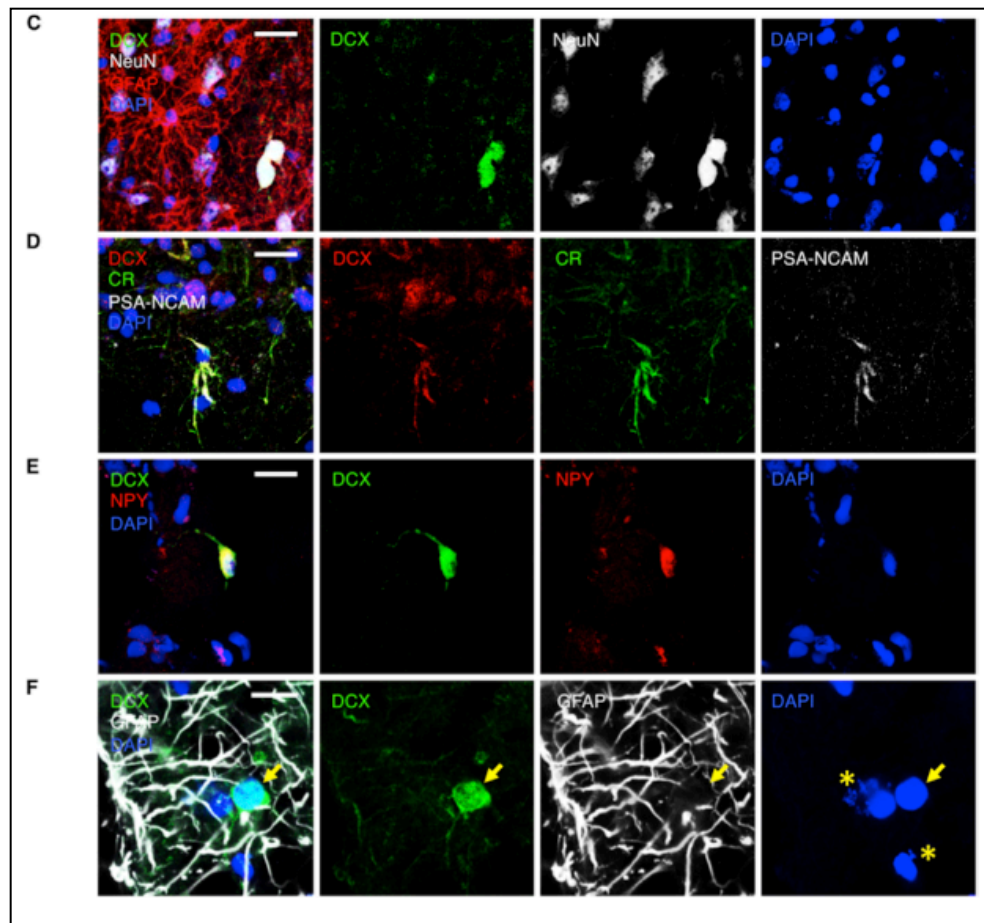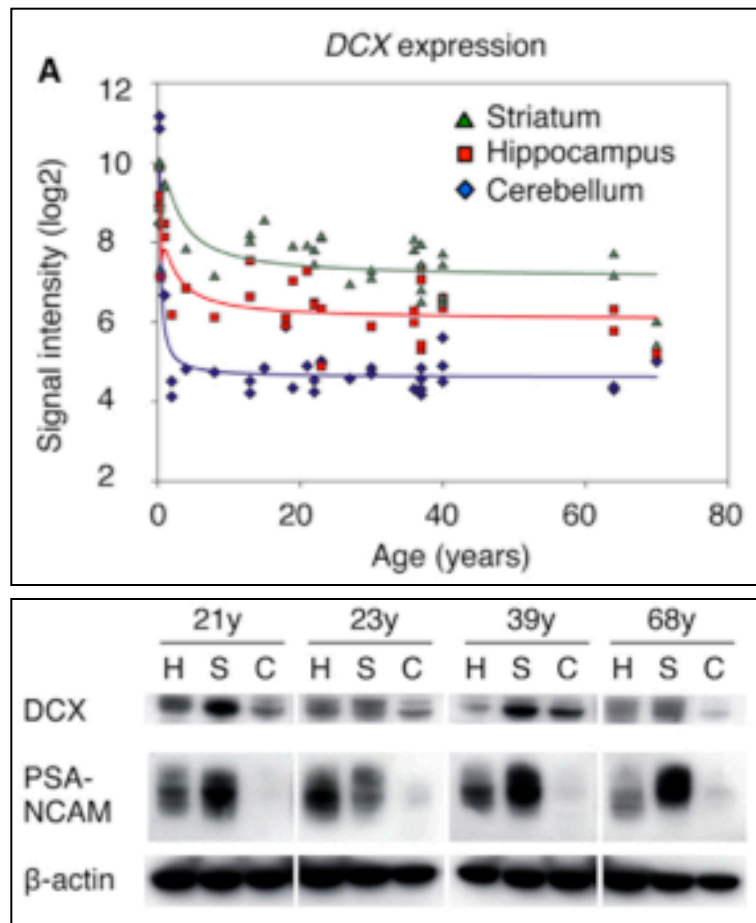
(A) DCX expression in the striatum (green), hippocampus (red), and cerebellum (blue) across the human lifespan. Data from Kang et al. (2011). The striatal area used for the transcriptome analysis comprises the caudate nucleus (lateral ventricle wall included), the nucleus accumbens, and the putamen. See also Table S1.
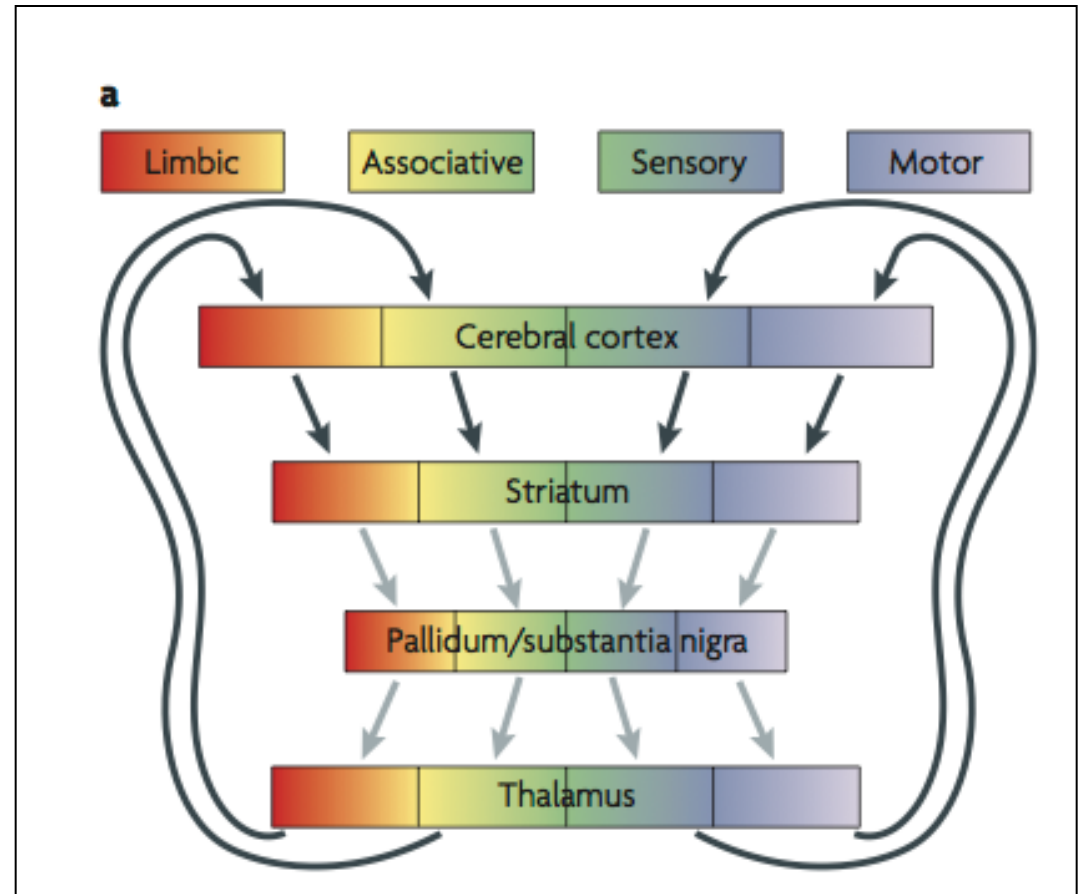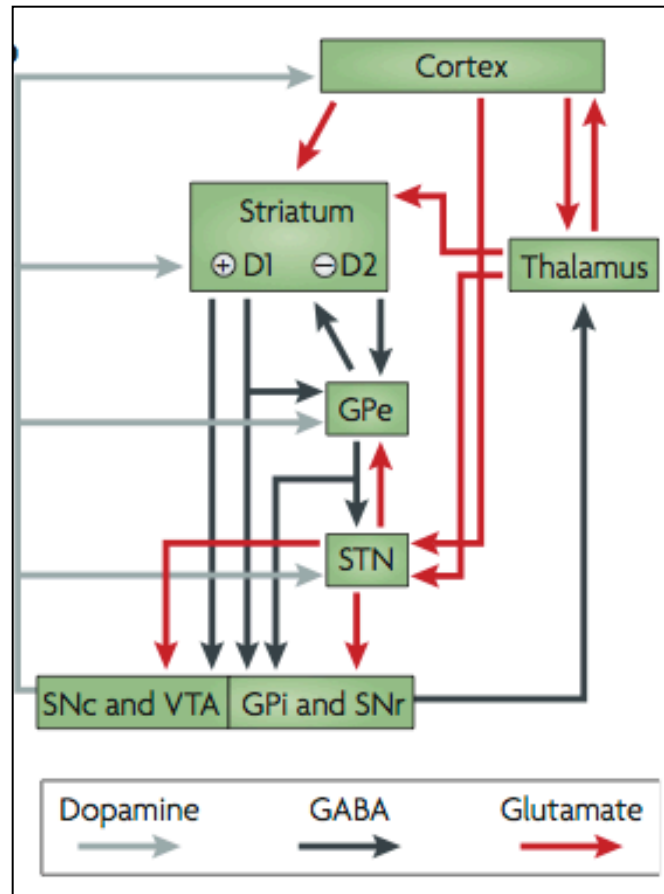
(B) Western blot analysis of DCX, PSA-NCAM and β-actin in the hippocampus (H), striatum (S), and cerebellum (C) of human subjects of different ages.

(C–F) Confocal microscopy of DCX-positive cells in the striatum. The majority of the DCX-positive cells express the mature neuronal marker NeuN but all of them lack expression of the astrocytic marker GFAP (C). Most of the DCX-positive cells also express PSA-NCAM (D). DCX occasionally colocalizes with neuronal markers calretinin (CR) (D) and NPY (E). Most DCX-positive cells have little or no lipofuscin (arrow), whereas the majority of DCX-negative cells contain lipofuscin pigments (stars) (F). Autofluorescent lipofuscin pigments are not visible in all channels because an antiautofluorescence treatment was applied. Scale bars, 20 μm for (C)–(E) and 10 μm for (F). Cell nuclei are labeled with DAPI and appear blue.

Goal-directed and habitual control in the basal ganglia: implications for Parkinson's disease
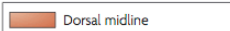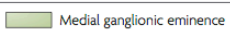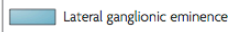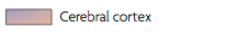
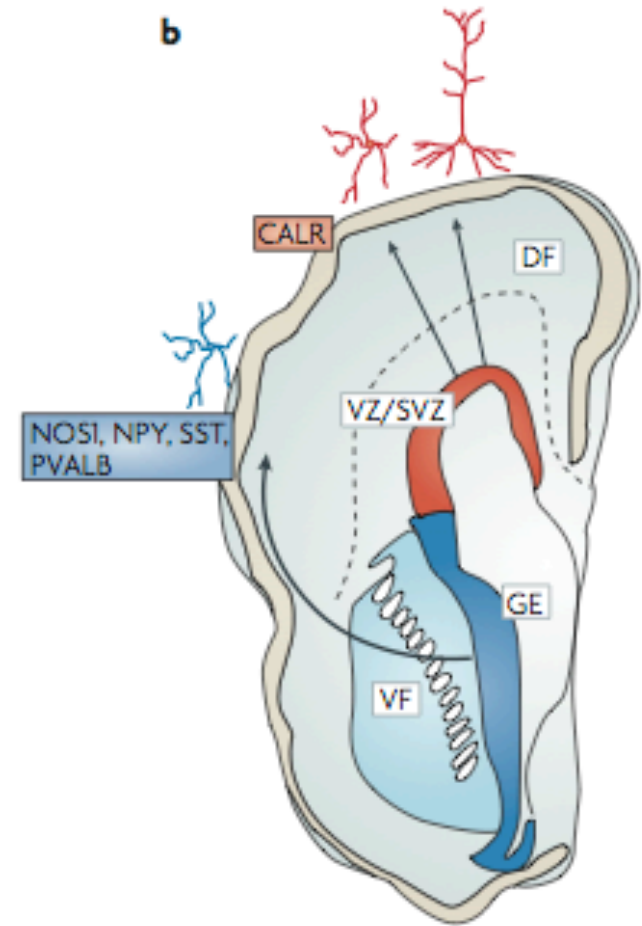Redgrave P, Rodriguez M, Smith Y, Rodriguez-Oroz MC, Lehericy S, Bergman H, Agid Y, Delong M, Obeso JA
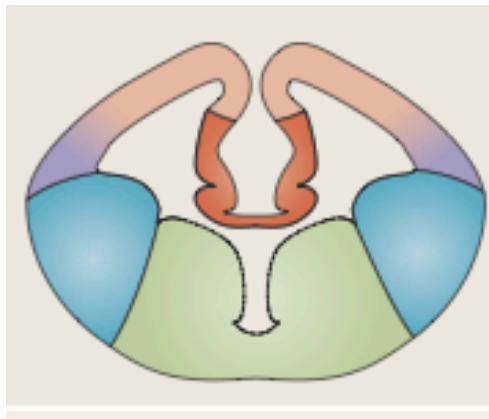
The genetics of early telencephalon patterning: some assembly required

Hébert J, Fishell G
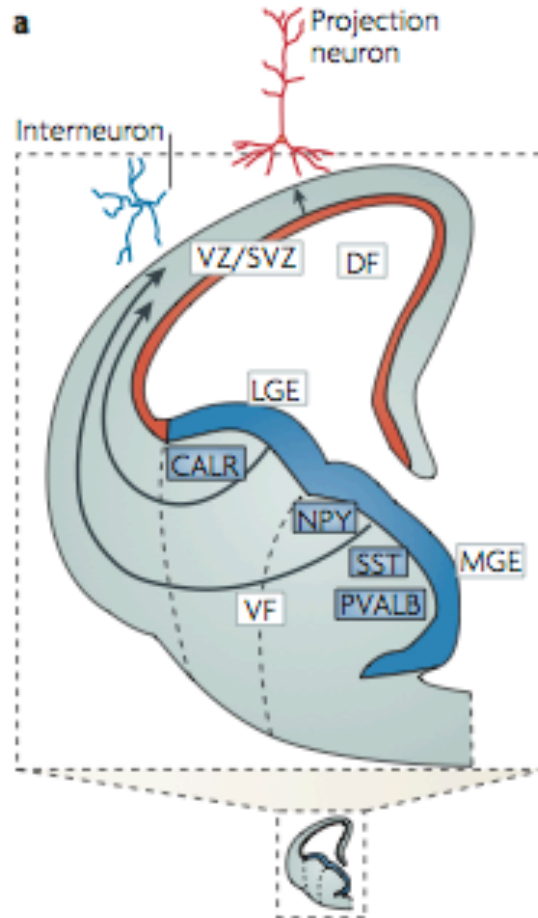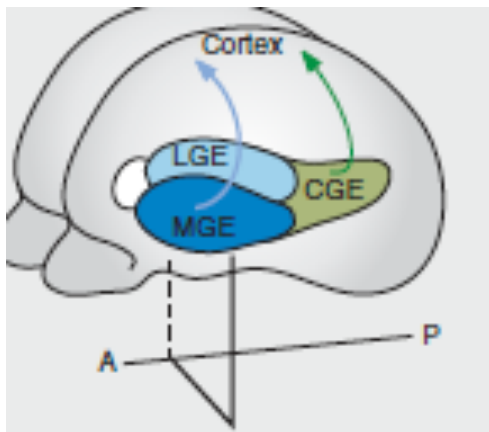
Interneuron cell types are fit to function

Kepecs A, Fishell G
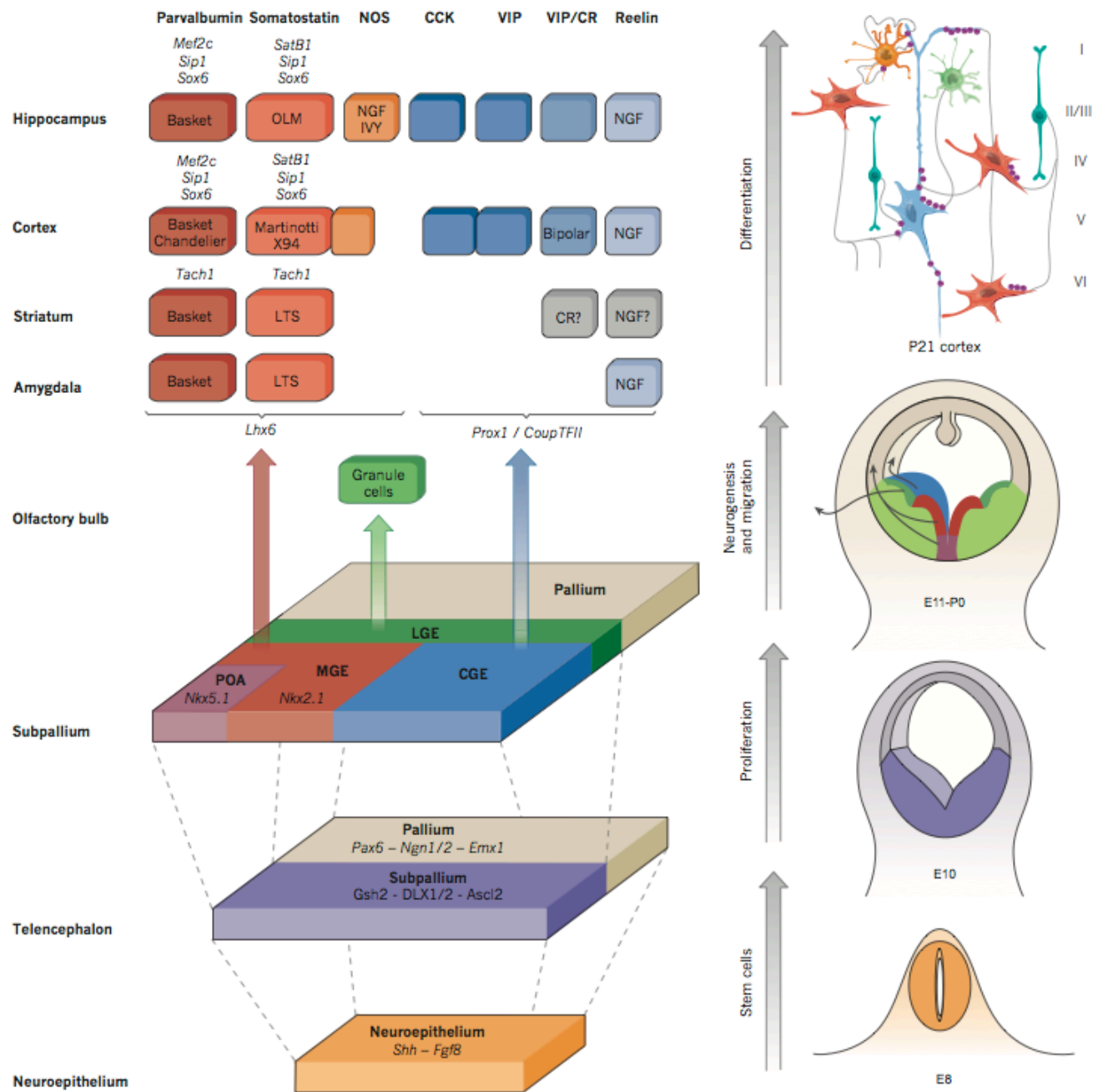
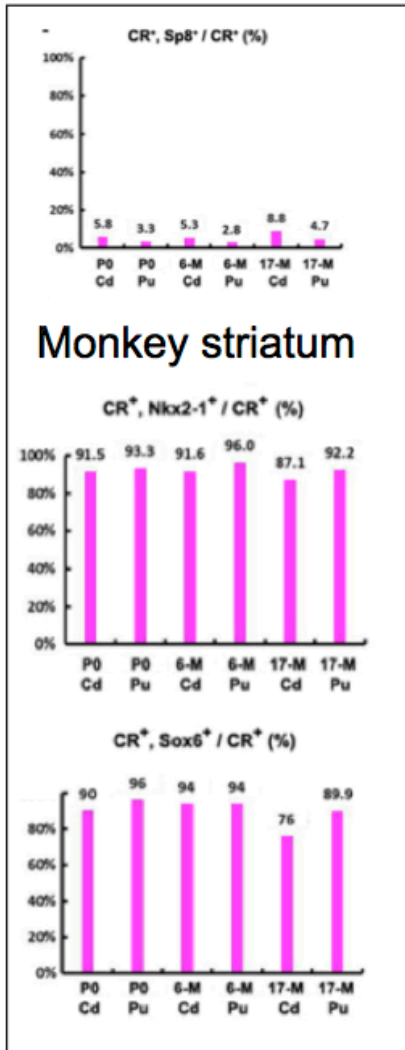# Human and Monkey Striatal Interneurons Are Derived from the Medial Ganglionic Eminence But Not from the Adult Subventricular Zone

Congmin Wang,[1,2]* Yan You,[1]* Dashi Qi,[1,3]* Xing Zhou,[1] Lei Wang,[4] Song Wei,[1] Zhuangzhi Zhang,[1] Weixi Huang,[1] Hong Liu,[1] Fang Liu,[1] Lan Ma,[1] and Zhengang Yang[1]

Chez le singe comme chez l'humain, les cellules du bulbe expriment Sp8 marqueur LGE/SVZ alors que les cellules du striatum expriment Sox6 et Nkx2.1, marqueurs de la MGE
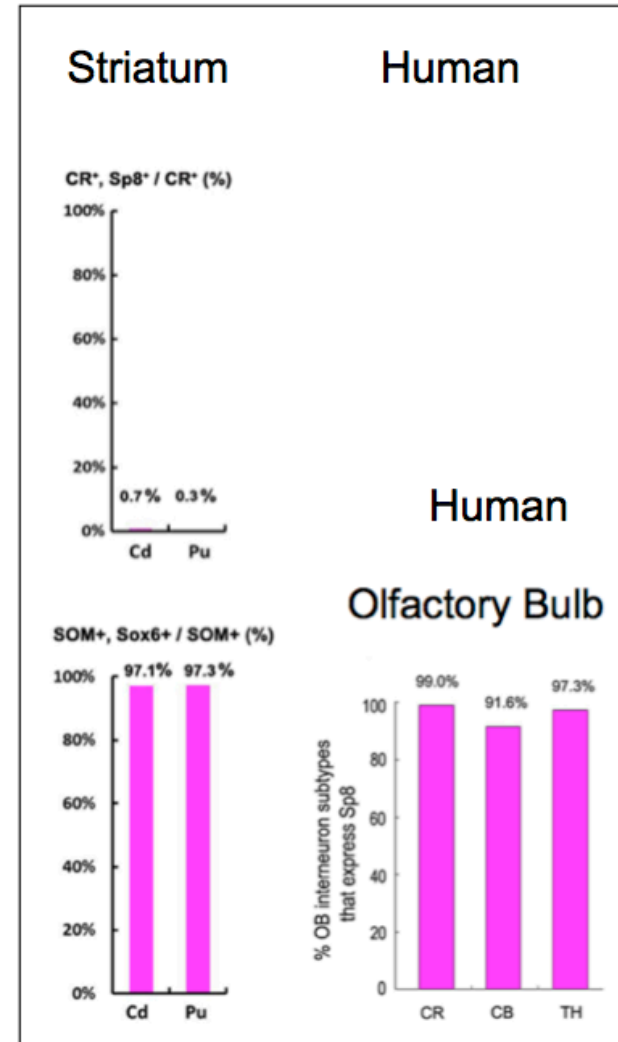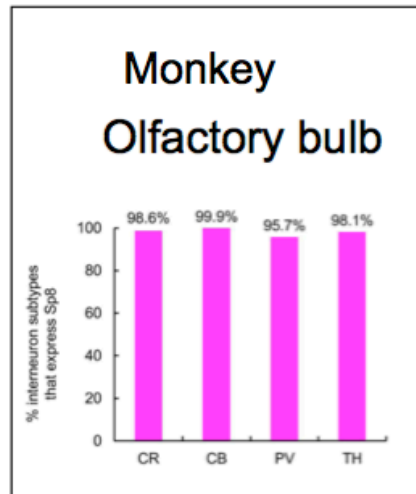
Human and Monkey Striatal Interneurons Are Derived from the Medial Ganglionic Eminence But Not from the Adult Subventricular Zone

Congmin Wang,[1,2]* Yan You,[1]* Dashi Qi,[1,3]* Xing Zhou,[1] Lei Wang,[4] Song Wei,[1] Zhuangzhi Zhang,[1] Weixi Huang,[1] Zhidong Liu,[1] Fang Liu,[1] Lan Ma,[1] and Zhengang Yang[1]
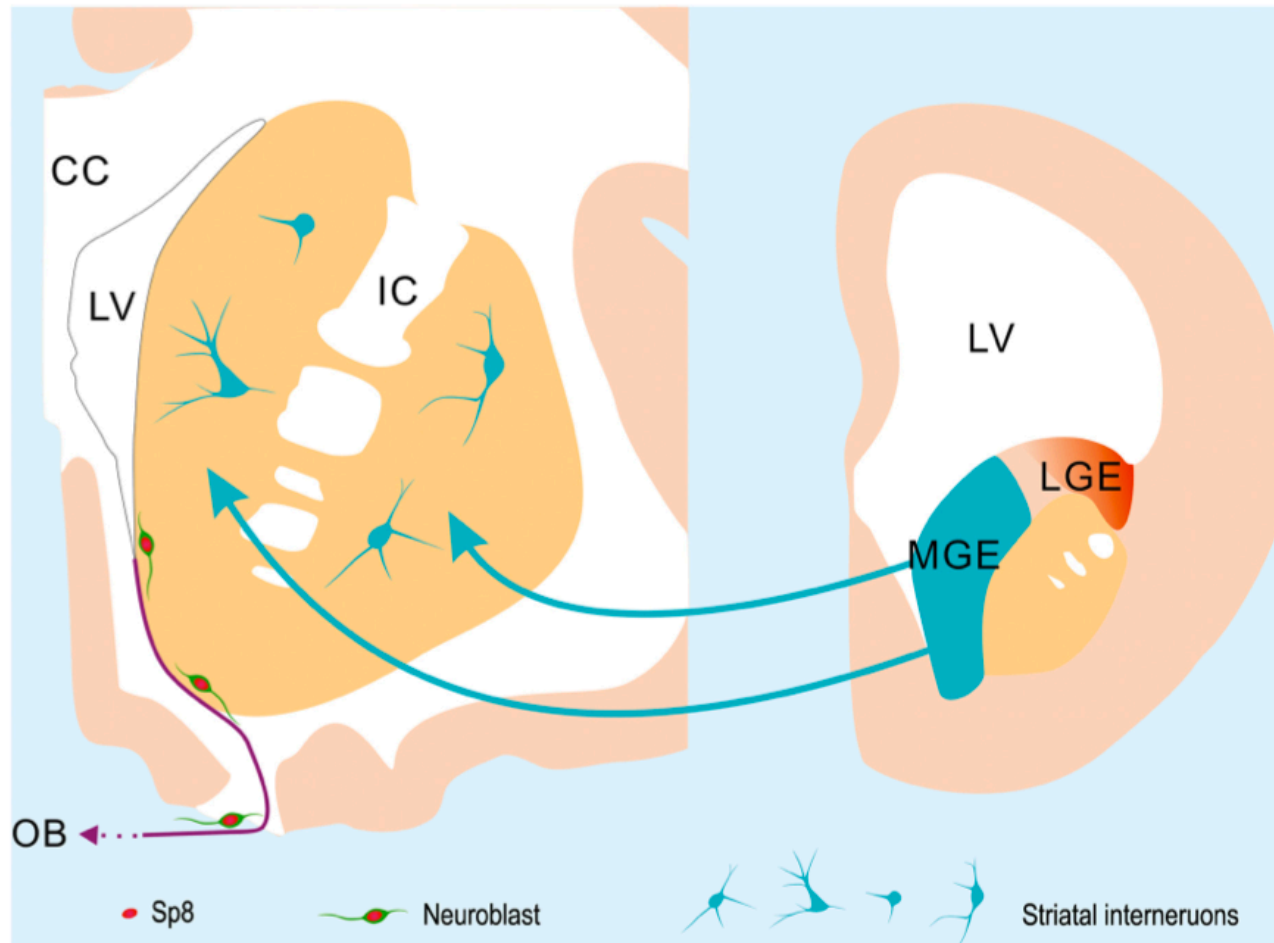

Figure 16. Proposed model for the origin of striatal interneurons in the human and monkey brain. The vast majority of interneurons in the adult human and monkey striatum are derived from the MGE during embryonic developmental stages. Very few neuroblasts are observed in the adult human SVZ and RMS. These neuroblasts express the transcription factor Sp8 and are likely destined for the OB, as they are in adult monkeys and rodents. Neuroblasts were not observed in the adult human striatum in our study.

Off the beaten track: new neurons in the adult human striatum
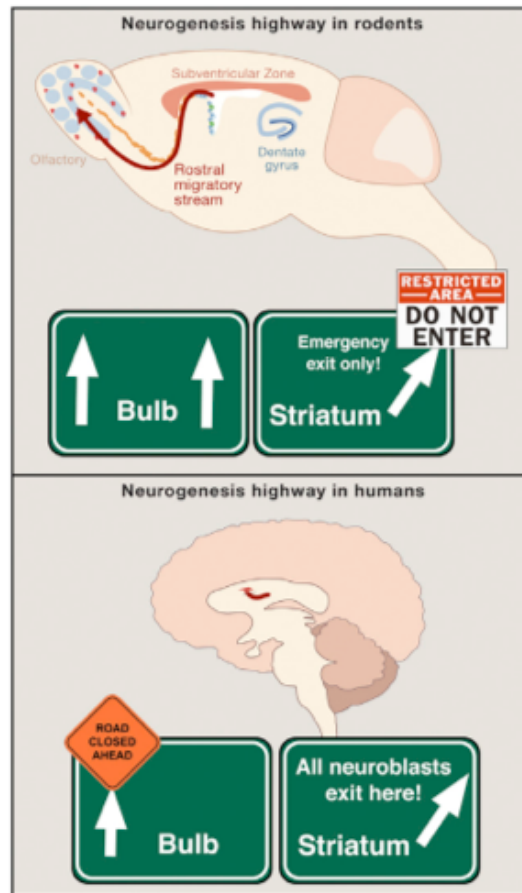
Kempermann G

Figure 1. Striatal Neurogenesis in Humans
Whereas neuroblasts from the adult subventricular zone (SVZ) in rodents migrate to the olfactory bulb to become interneurons, and enter the striatum only under pathological conditions such as ischemia (top), in humans hardly any adult neurogenesis can be found in the adult olfactory bulb, but it occurs to substantial degree in the striatum (Ernst et al., 2014).

Dynamics of hippocampal neurogenesis in adult humans

Spalding KL, Bergmann O, Alkass K, Bernard S, Salehpour M, Huttner HB, Boström E, Westerlund I, Vial C, Buchholz BA, Possnert G, Mash DC, Druid H, Frisén J

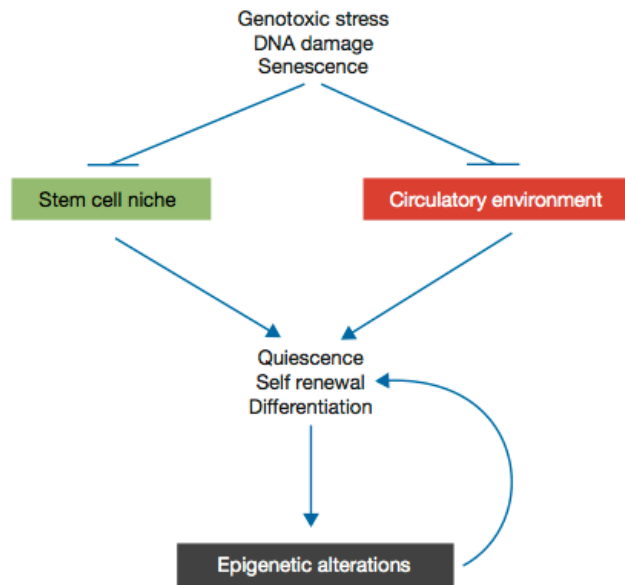mature neurons in experimental animals are not readily applicable to humans. To be able to study cell turnover dynamics in humans, we have developed a strategy to retrospectively birth date cells (Spalding et al., 2005a). This strategy takes advantage of the elevated atmospheric ^{14}C levels caused by above-ground nuclear bomb testing in 1955–1963 during the Cold War (De Vries, 1958; Nydal and Lövseth, 1965). Since the Partial Nuclear Test Ban Treaty in 1963, atmospheric levels of ^{14}C have declined because of uptake by the biotope and diffusion from the atmosphere (Levin and Kromer, 2004; Levin et al., 2010). ^{14}C in the atmosphere reacts with oxygen to form CO_2, which is taken up by plants in photosynthesis. When we eat plants, or animals that live off plants, we take up ^{14}C, meaning that atmospheric ^{14}C levels are mirrored in the human body at all times (Harkness, 1972; Libby et al., 1964; Spalding et al., 2005b). When a cell goes through mitosis and duplicates its chromosomes, it integrates ^{14}C in the synthesized genomic DNA with a concentration corresponding to that in the atmosphere at the time, creating a date mark in the DNA (Spalding et al., 2005a). The cumulative nature of ^{14}C integration makes the method especially suited for establishing the kinetics of slowly turning over cell populations. The accuracy of individual datings is approximately ±1.5 years (Spalding et al., 2005b), but higher accuracy is reached by integrating data from many independent measurements.

Impact of genomic damage and ageing on stem cell function

Behrens A, van Deursen JM, Rudolph KL, Schumacher B

Figure 2 Impact of DNA damage on the stem cell environment. The accumulation of DNA damage and senescent cells during ageing leads to alterations in the stem cell niche and the systemic circulatory environment. Both processes can interfere with signalling pathways (such as Notch, Wnt and Sprouty1) that are required for the maintenance of stem cell quiescence, self-renewal and differentiation. Disturbances in these basic stem cell parameters lead to alterations in the epigenetic landscape of the DNA of ageing stem cells, further aggravating alterations in stem cell quiescence, self-renewal and differentiation.

Notch signalling in vertebrate neural development
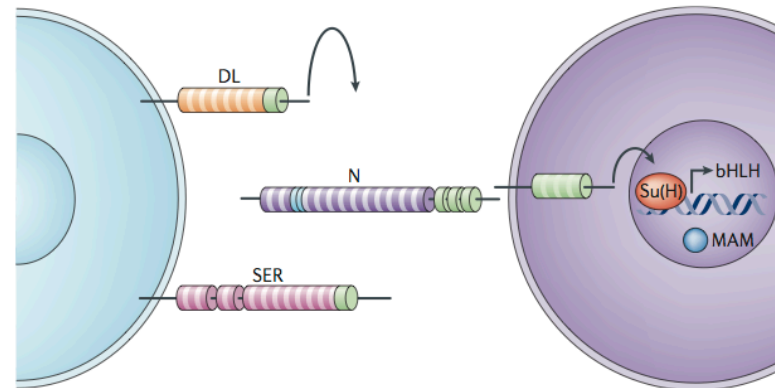
Louvi A, Artavanis-Tsakonas S

Figure 2 | **The core of the Notch signalling pathway.** Shows the receptor (N) on the surface of one cell and the ligands delta (DL) and serrate (SER) on the surface of an adjacent cell. On interaction of the receptor with a ligand (arrow), a series of proteolytic events eventually release the intracellular domain from the cell surface, allowing it to translocate to the nucleus, where it associates with the DNA-binding effector suppressor of hairless (Su(H)) and the nuclear protein mastermind (MAM). This complex is essential for triggering the transcription of target genes, with the basic helix–loop–helix (bHLH) proteins a key class among such targets. Modified, with permission, from REF. 42 © (1999) American Association for the Advancement of Science.

Pax7 is critical for the normal function of satellite cells in adult skeletal muscle

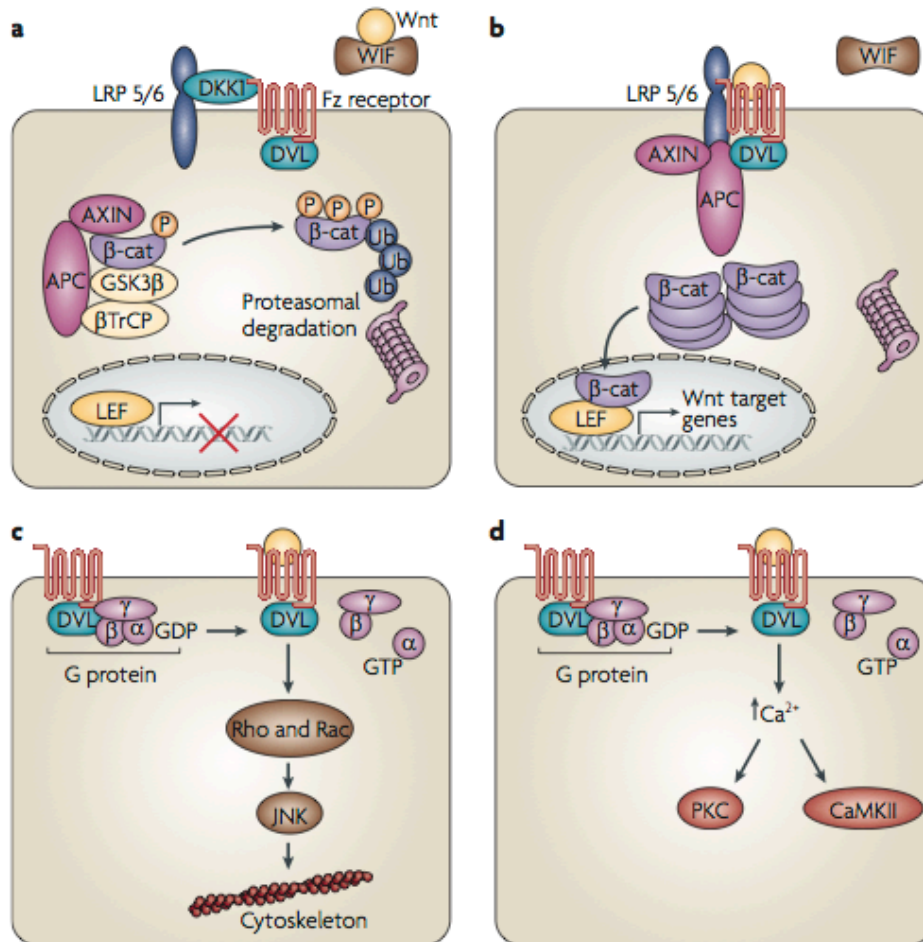# Emerging roles of Wnts in the adult nervous system

Inestrosa NC, Arenas E

Figure 1 | **The Wnt signalling pathways. a** | Canonical Wnt signalling is inhibited in the presence of DKK1. Under these conditions glycogen synthase kinase 3β (GSK3β) is activated and β-catenin (β-cat) phosphorylated and eventually degraded in the proteasome. **b** | When canonical Wnt signalling is activated, the Wnt ligand interacts with Frizzled (Fz) receptors and the co-receptor low-density lipoprotein receptor-related protein 5 (LRP5)/LRP6. Under these conditions GSK3β is blocked and β-catenin accumulates in the cytoplasm before moving into the nucleus, where it activates the transcription of Wnt target genes. **c** | In non-canonical Wnt–Jun N-terminal kinase (JNK) signalling the activation of Fz receptors, Dishevelled (DVL) and the monomeric GTPases Rho and Rac activates JNK. This facilitates the interaction of JNK with the cytoskeleton, or activates transcription through AP-1 (not shown). **d** | In non-canonical Wnt–Ca^{2+} signalling activation of Fz and DVL increases the intracellular Ca^{2+} concentration, which in turn activates both protein kinase C (PKC) and calcium/calmodulin-dependent protein kinase II (CaMKII); these kinases can then modify different signalling components, including postsynaptic receptors. In both cases of non-canonical Wnt signalling, evidence suggests that G proteins are probably involved in the transduction of the Wnt signal. βTrCP, transducin repeat-containing protein; APC, adenomatous polyposis coli; LEF, lymphoid enhancer-binding factor (also known as T cell factor); Ub, ubiquitin; WIF, Wnt inhibitory factor.

Non canonique

Impact of genomic damage and ageing on stem cell function

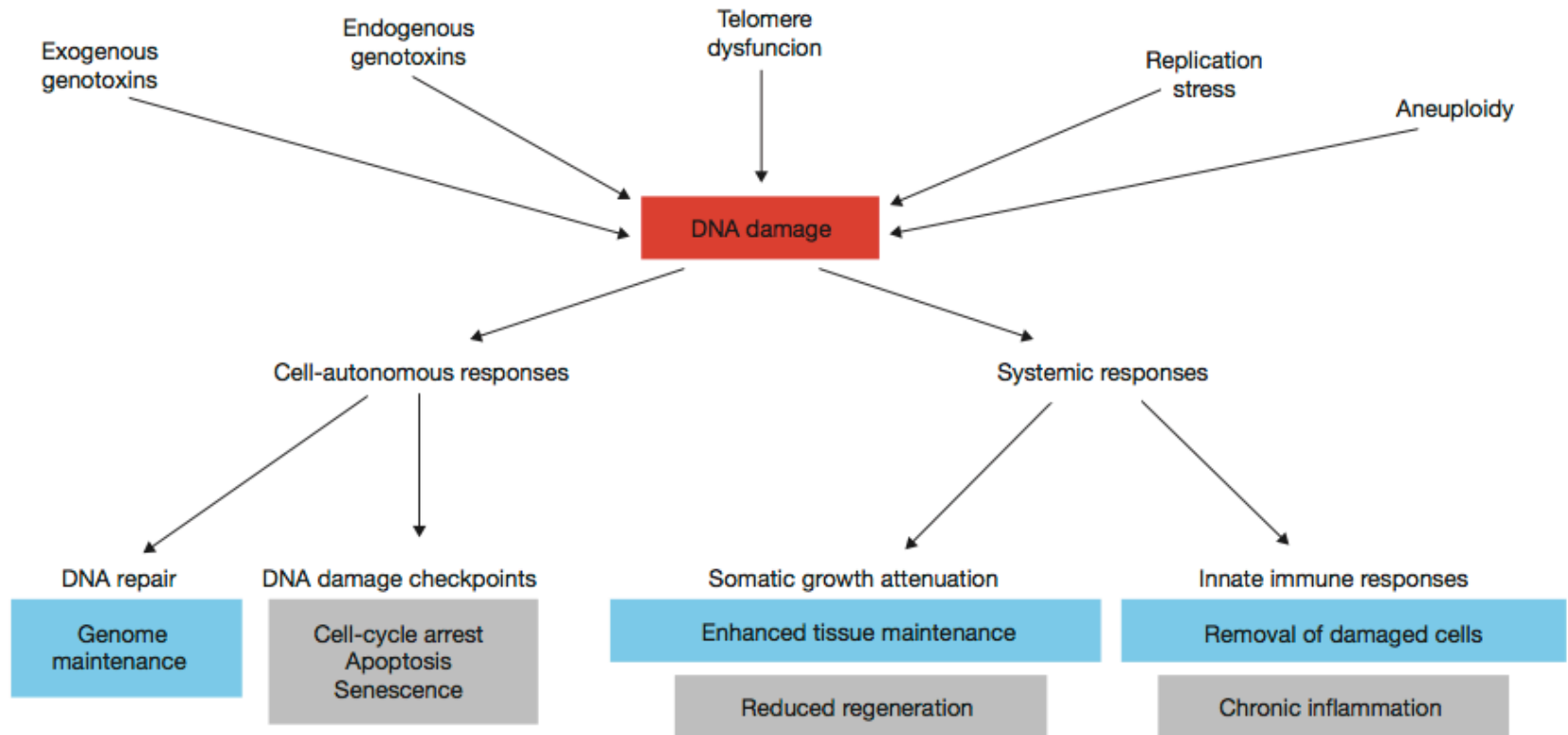Behrens A, van Deursen JM, Rudolph KL, Schumacher B

Figure 1 Cell-autonomous and systemic responses to DNA damage. Various sources of genotoxic stress induce DNA damage that can be removed by specialized DNA repair systems. Cell-autonomous DNA damage checkpoints halt the cell cycle to allow time for repair or, amid severe genome damage, trigger programmed cell death or cellular senescence. Although DNA damage checkpoint mechanisms protect against cancer, the associated removal of cells can contribute to ageing through declining regenerative stem cell pools (grey). Systemic DNA damage responses include attenuation of the somatic growth axis and triggering of innate immune responses, which might support longevity assurance (blue) by enhancing maintenance of tissue functionality and removal of damaged cells, but also contribute to ageing (grey) by damaging tissues and impairing regeneration.

Modifying IGF1 activity: an approach to treat endocrine disorders, atherosclerosis and cancer
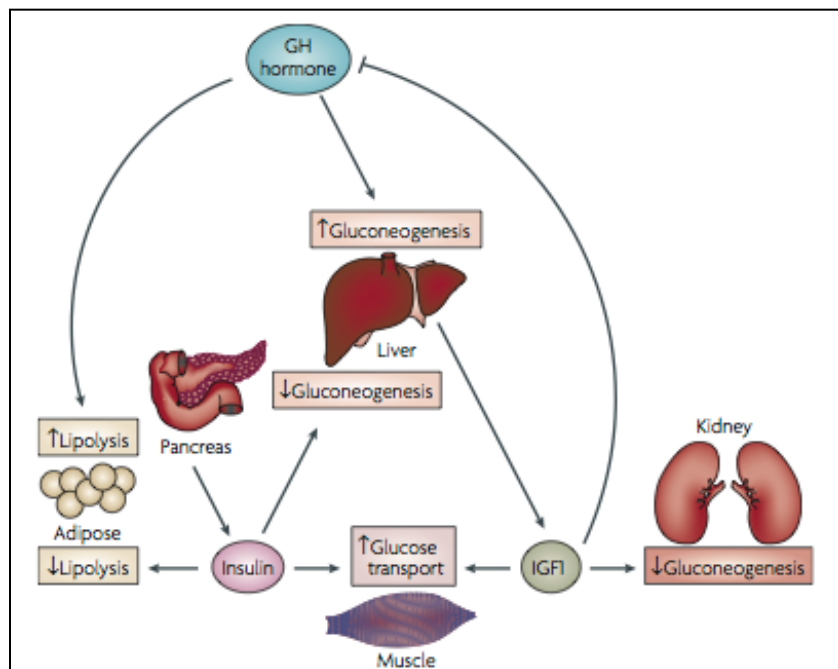
David R. Clemmons

Figure 2 | **Growth hormone and IGF1 actions on glucose homeostasis.** In addition to growth stimulation, growth hormone (GH) and insulin-like growth factor 1 (IGF1) have many important metabolic actions. GH acts directly on the liver to antagonize the ability of insulin, which is secreted by the pancreas, to inhibit gluconeogenesis. GH acts directly on fat cells to enhance lypolysis, which functions to elevate blood glucose, again antagonizing the effects of insulin. IGF1 can directly lower blood glucose by inhibiting renal gluconeogenesis. IGF1 can also act indirectly, through the IGF1 receptor in skeletal muscle, to enhance insulin action on glucose transport. IGF1 inhibits GH secretion by the pituitary gland, thus, IGF1 indirectly blocks the ability of GH to antagonize insulin action; this indirect effect improves glucose homeostasis.
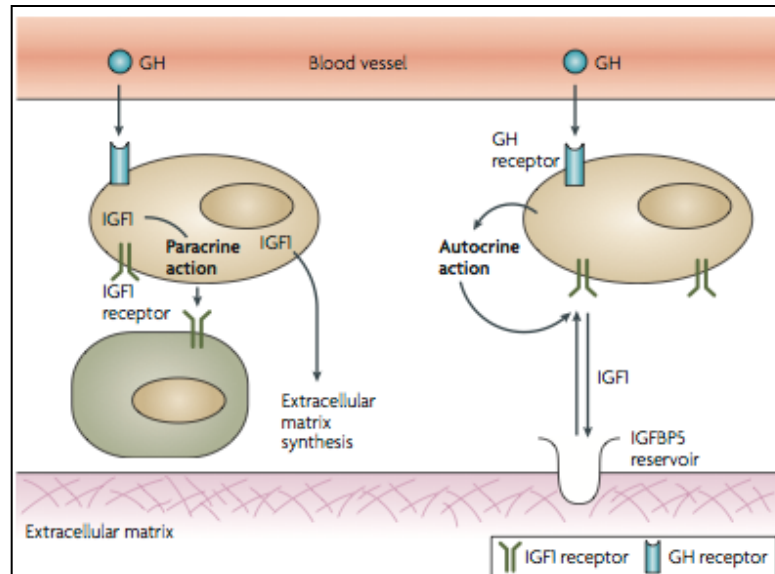

Figure 1 | **Autocrine and paracrine actions of IGF1.** Insulin-like growth factor 1 (IGF1) is synthesized in peripheral tissues by connective tissue cell types such as fibroblasts. These cells contain growth hormone receptors and can respond to growth hormone (GH) that enters the tissues from blood vessels. Newly synthesized IGF1 is secreted and transported to adjacent cells (paracrine action), where it stimulates coordinated cellular growth. It can also be secreted and then rebind to the cell of origin, where it stimulates cell growth (autocrine action). Similarly, locally produced IGF1 can bind to IGF binding proteins (IGFBPs) such as IGFBP5 localized in the extracellular matrix where a reservoir of IGF1, which can be released following tissue injury or during repair, is created. Stimuli other than GH, such as platelet-derived growth factor, can increase IGF1 synthesis; these factors are important for initiating the response of tissue repair after injury.
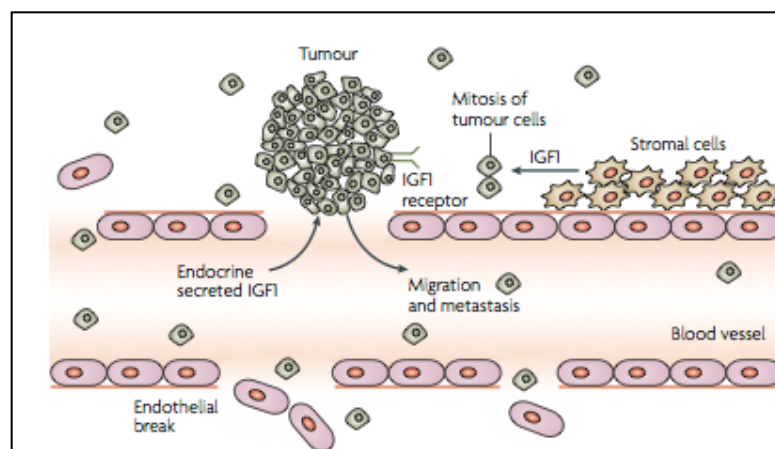
The Hallmarks of Aging

Carlos López-Otín,[1] Maria A. Blasco,[2] Linda Partridge,[3,4] Manuel Serrano,[5,*] and Guido Kroemer[6,7,8,9,10]

Figure 1. The Hallmarks of Aging
The scheme enumerates the nine hallmarks described in this Review: genomic instability, telomere attrition, epigenetic alterations, loss of proteostasis, deregulated nutrient sensing, mitochondrial dysfunction, cellular senescence, stem cell exhaustion, and altered intercellular communication.
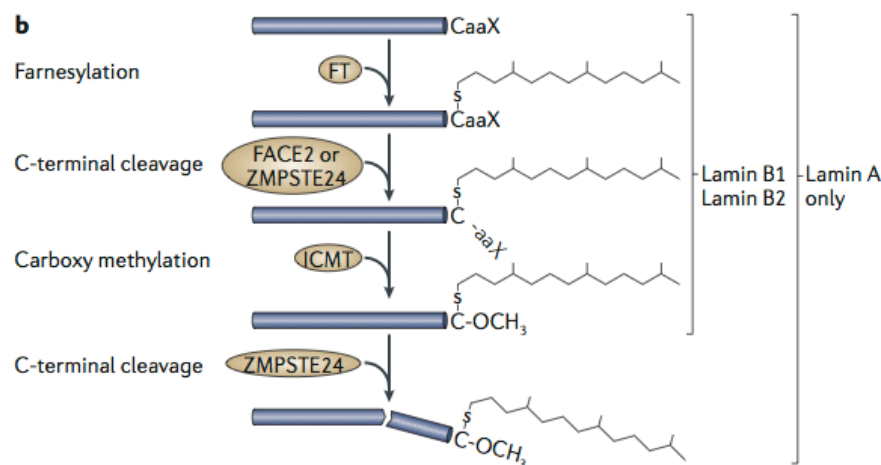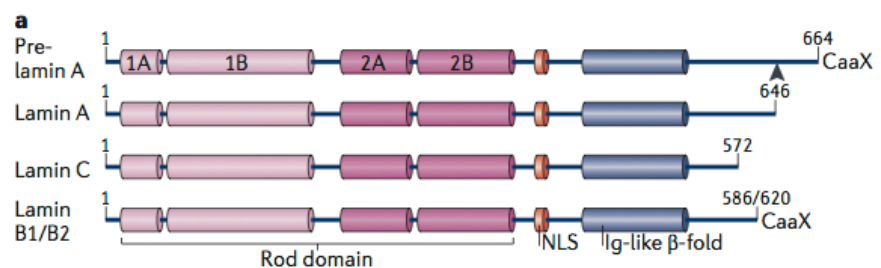
The nuclear lamins: flexibility in function

Burke B, Stewart CL

Institute of Medical Biology, 8A Biomedical Grove, Immunos 06–06, Singapore
138648. Brian.Burke@ imb.a-star.edu.sg

Progeria: a paradigm for translational medicine
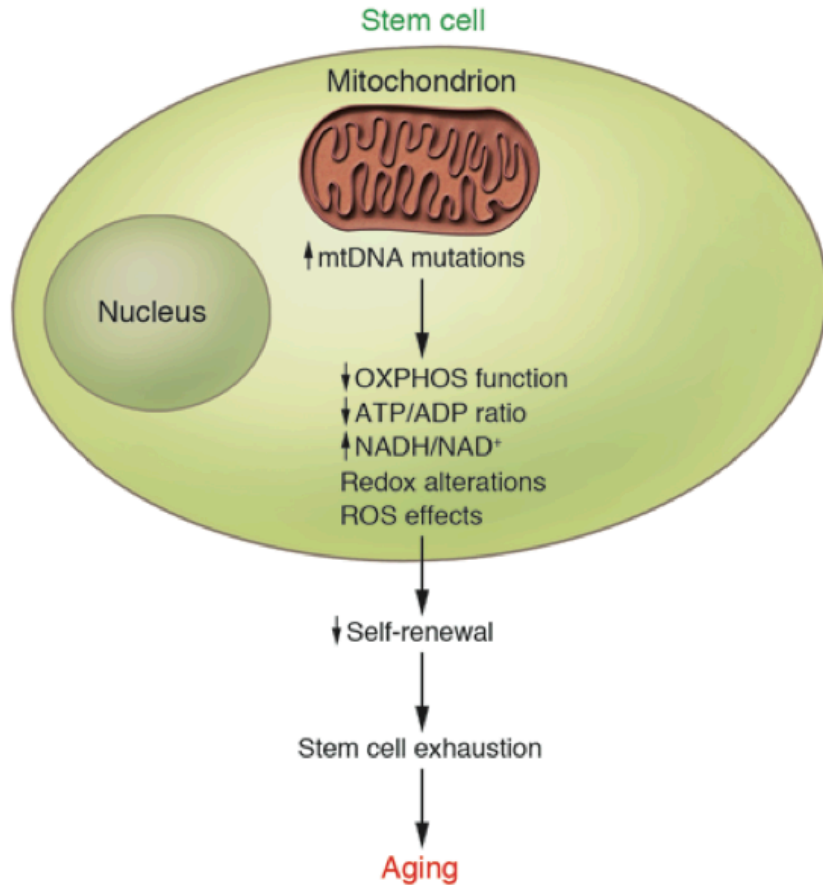
Gordon LB, Rothman FG, López–Otín C, Misteli T
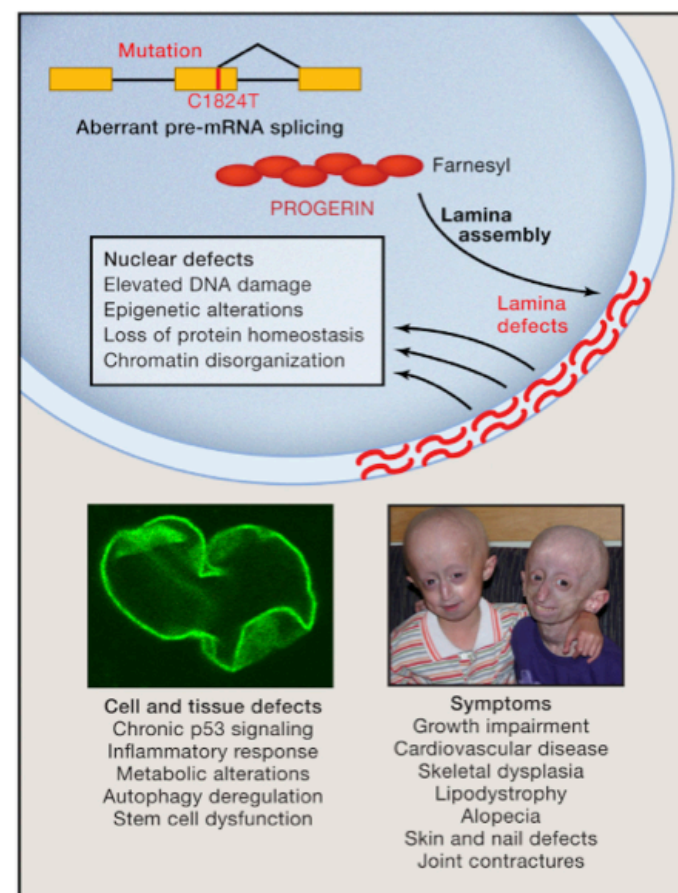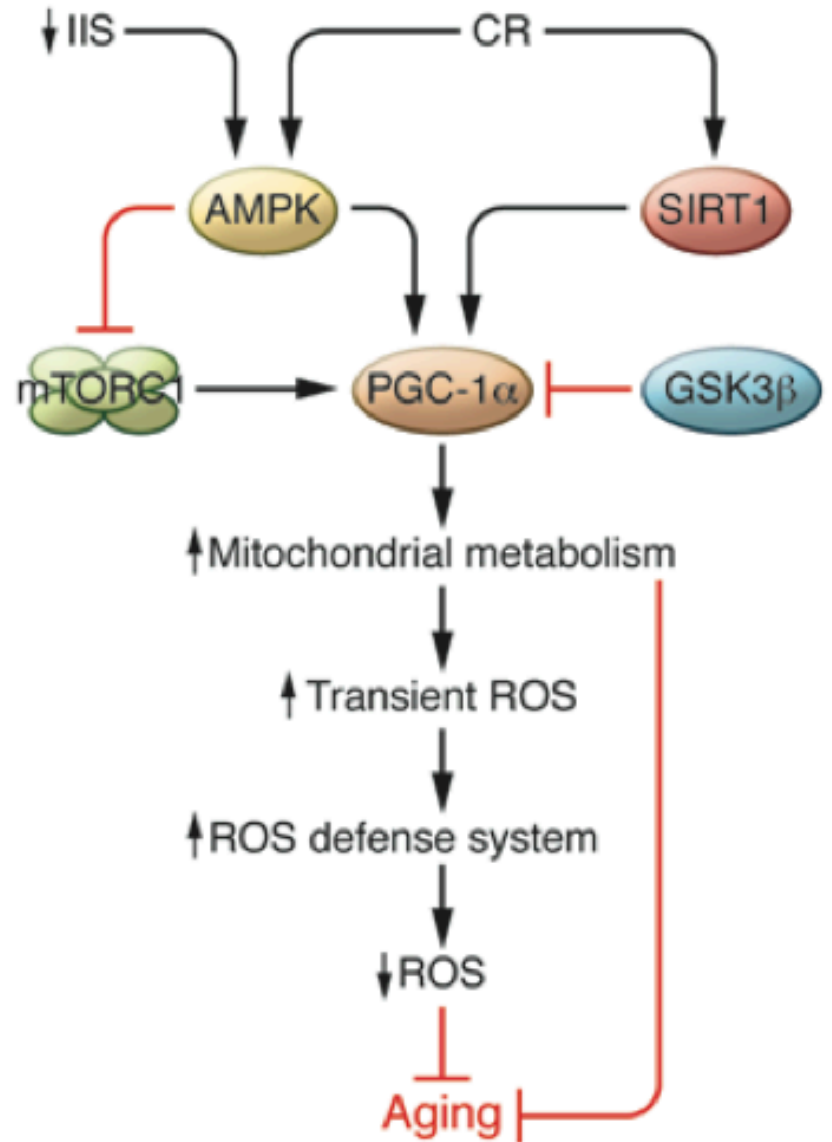
The role of mitochondria in aging

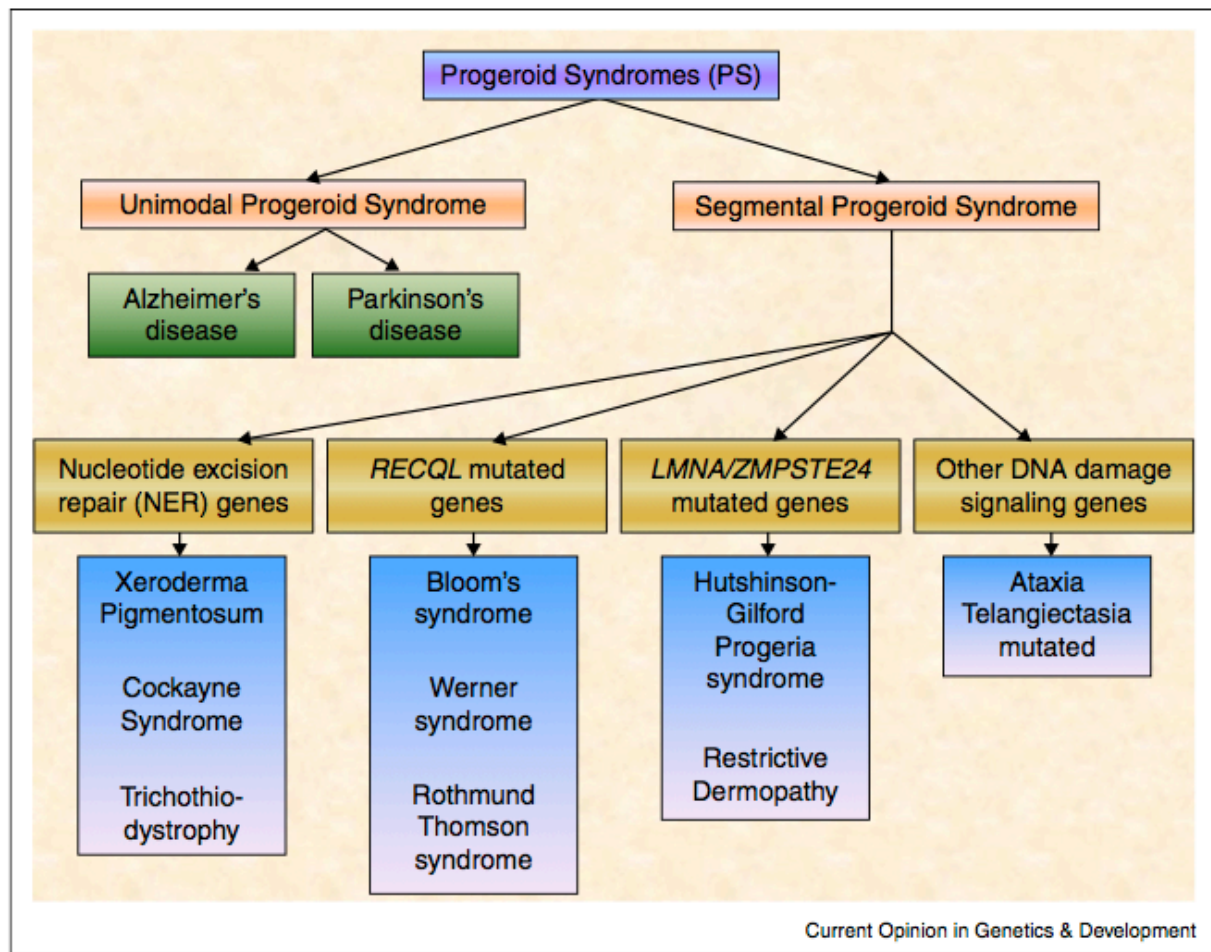Bratic A, Larsson N

J Clin Invest
2013 vol. 123 (3) pp. 951–7

nutrient sensing   calory restiction

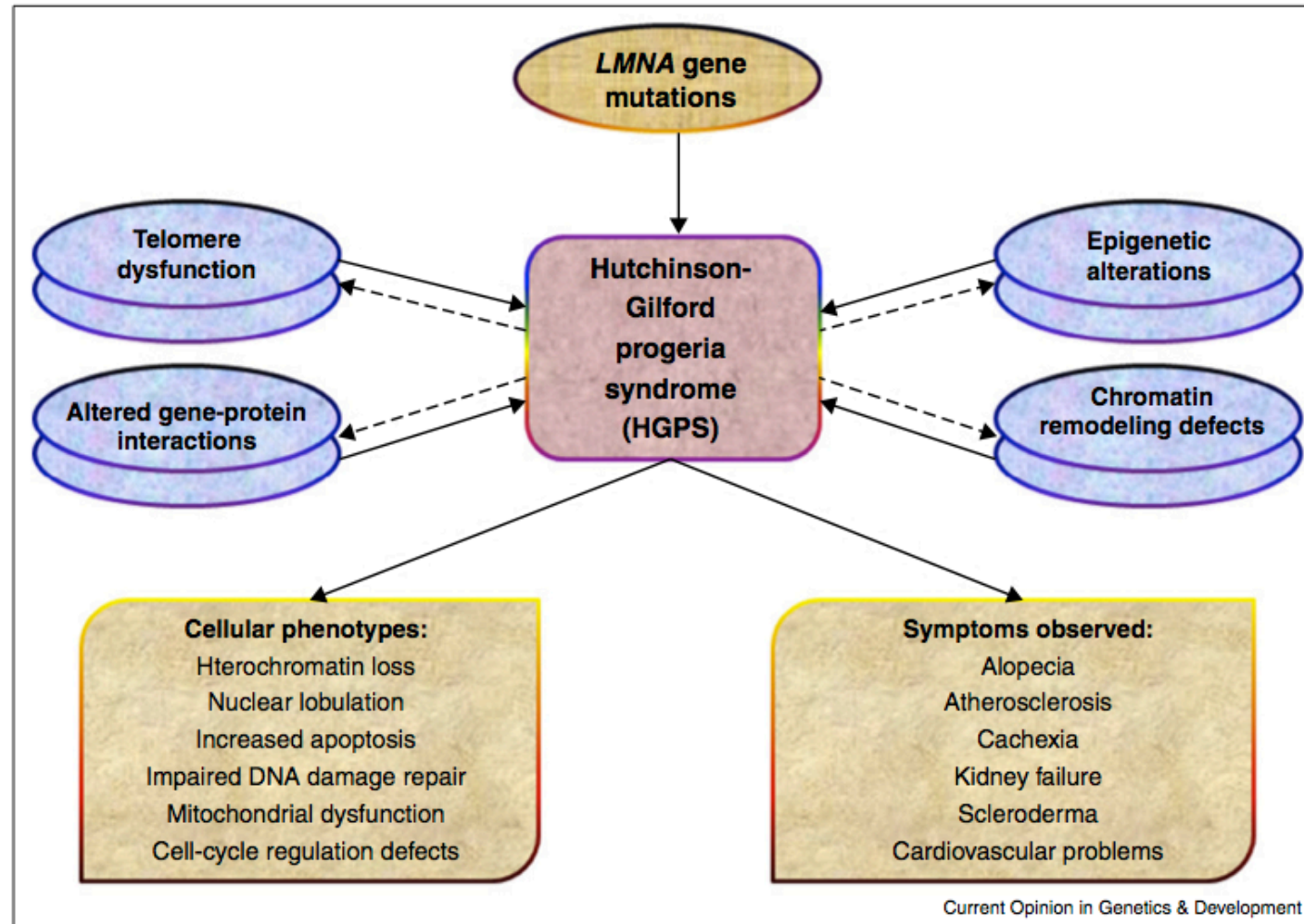# Genetics of aging, progeria and lamin disorders

Ghosh S, Zhou Z

Categorization of progeroid syndromes: progeroid syndromes can be broadly classified on the basis of number and type of affected tissues and also on the type of genes mutated/deleted.

Genetics of aging, progeria and lamin disorders

Ghosh S, Zhou Z

Defective genetic pathways and consequences of HGPS: several defects in different genetic pathways contribute to the cellular malfunctions and severe symptoms observed in Hutchinson–Gilford Progeria Syndrome patients.
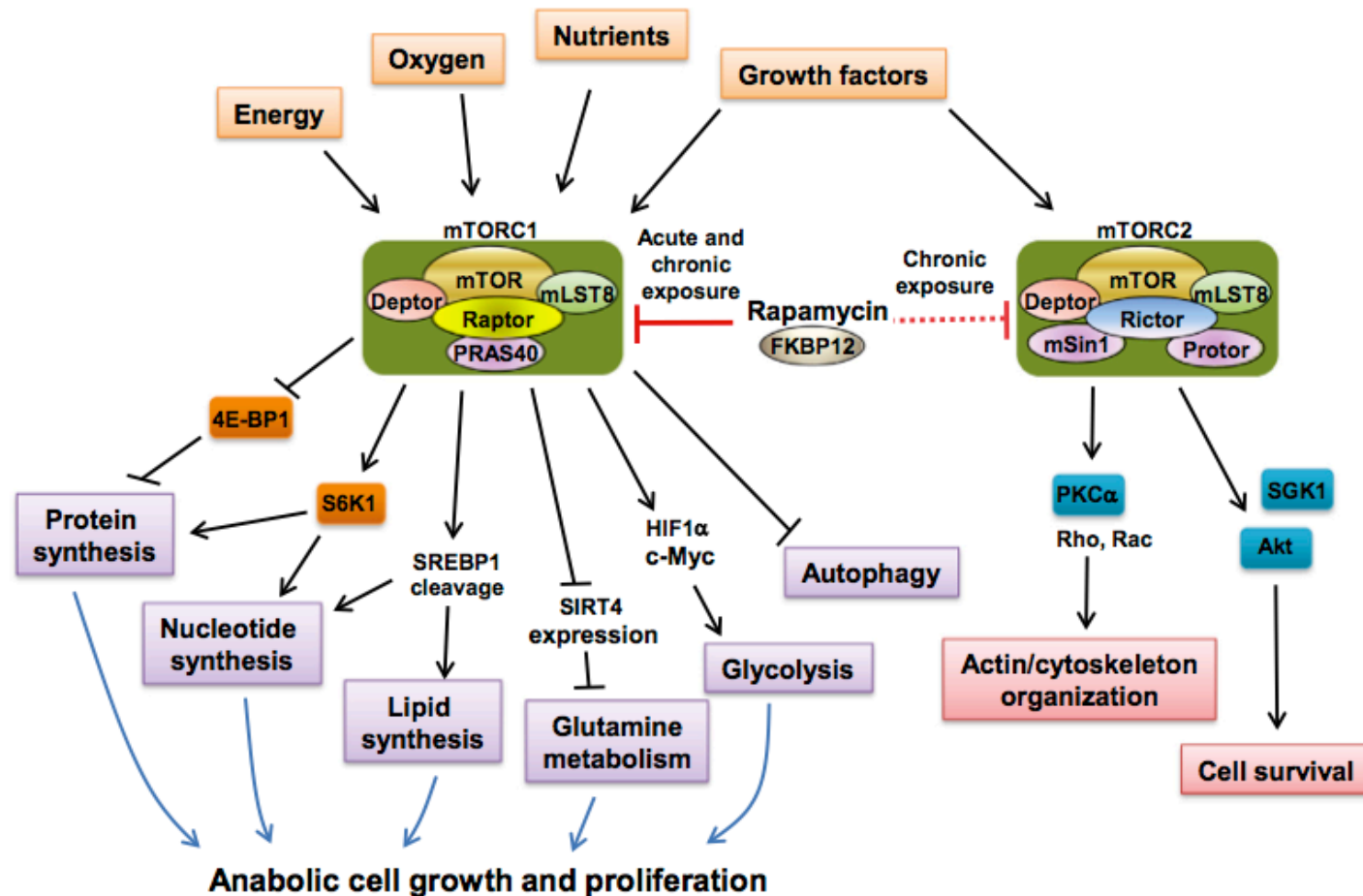
Rapamycin: One Drug, Many Effects
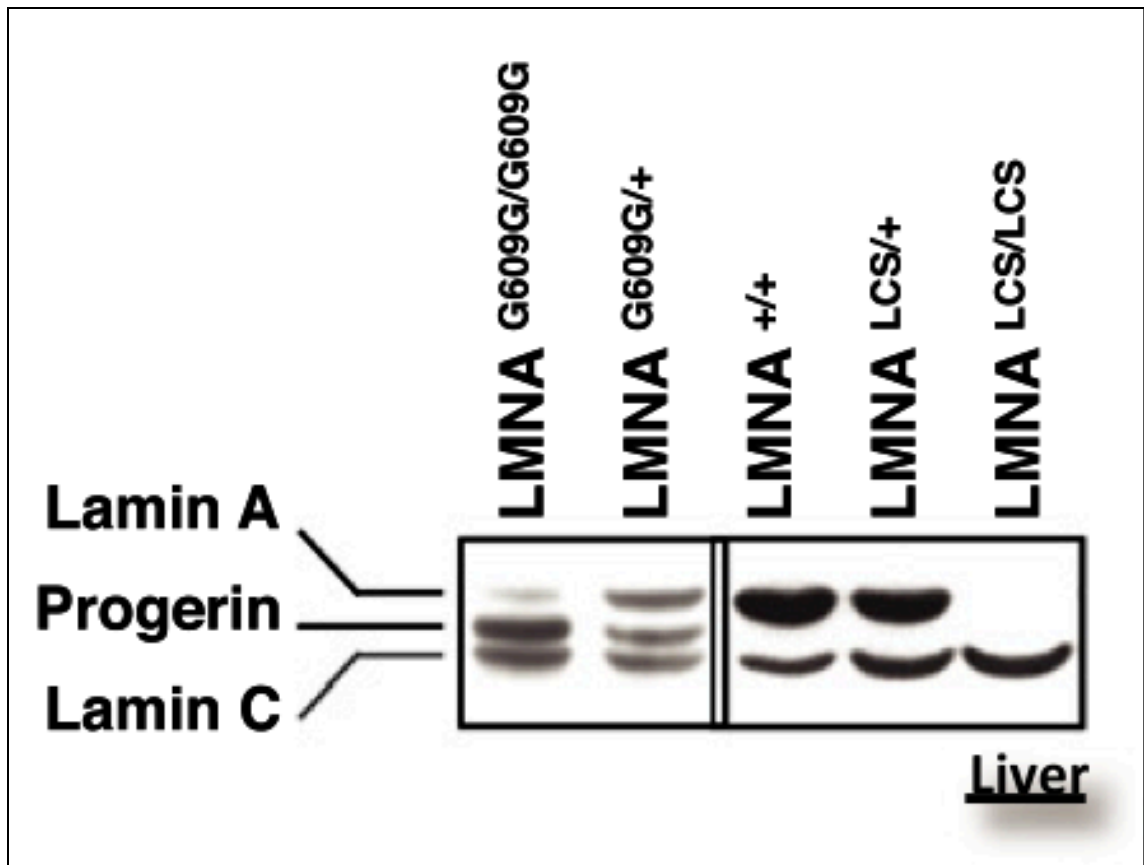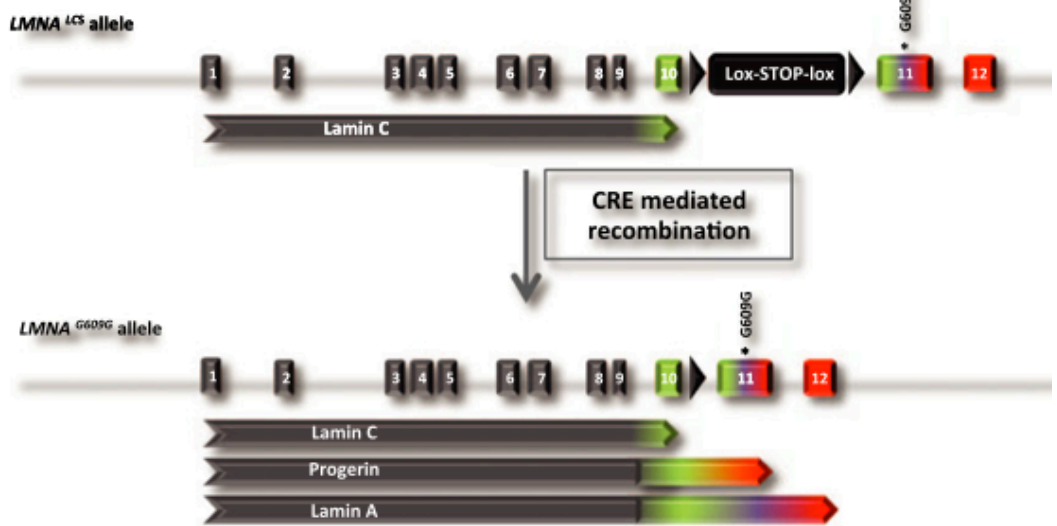
Li J, Kim SG, Blenis J

Figure 1. The Two mTOR Complexes and the Regulation of Key Cellular Processes
mTOR exists in two functionally distinct complexes, termed mTORC1 and mTORC2. mTORC1 integrates multiple signals from growth factors, oxygen, energy levels, and nutrients such as amino acids to promote cell growth and proliferation by activation of anabolic processes such as protein, lipid, and nucleotide synthesis; stimulation of energy metabolism such as glycolysis and glutaminolysis; and inhibition of catabolic process such as autophagy. Unlike mTORC1, mTORC2 only responds to growth factors and regulates actin/cytoskeleton organization and cell survival through the pathways as shown above. Rapamycin acutely inhibits mTORC1, whereas chronic exposure to rapamycin can also inhibit mTORC2.
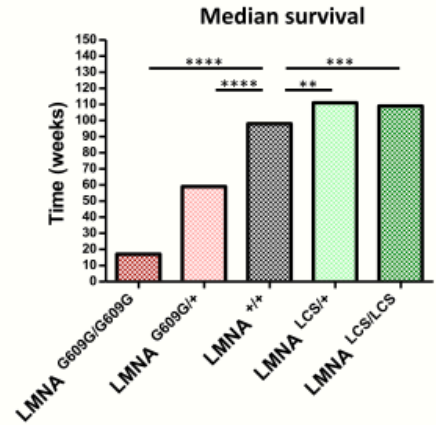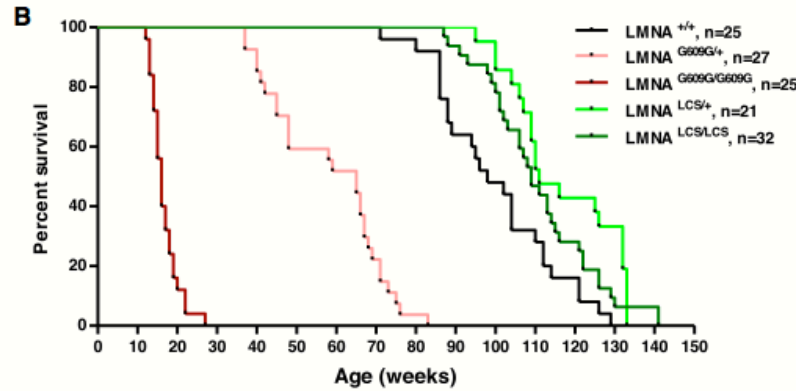
Antagonistic functions of LMNA isoforms in energy expenditure and lifespan

Lopez-Mejia IC, de Toledo M, Chavey C, Lapasset L, Cavelier P, Lopez-Herrera C, Chebli K, Fort P, Beranger G, Fajas L, Amri EZ, Casas F, Tazi J
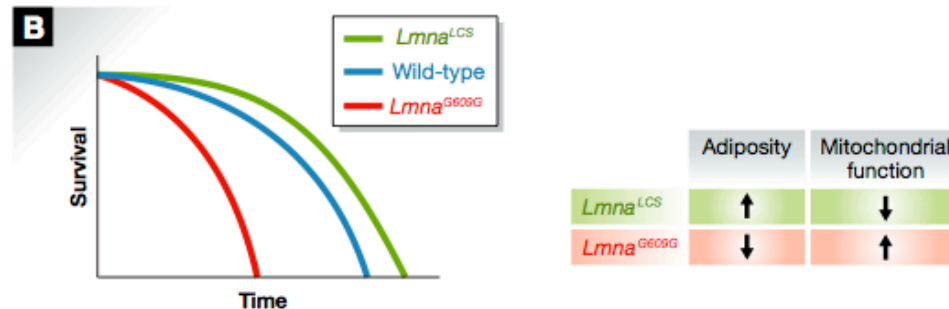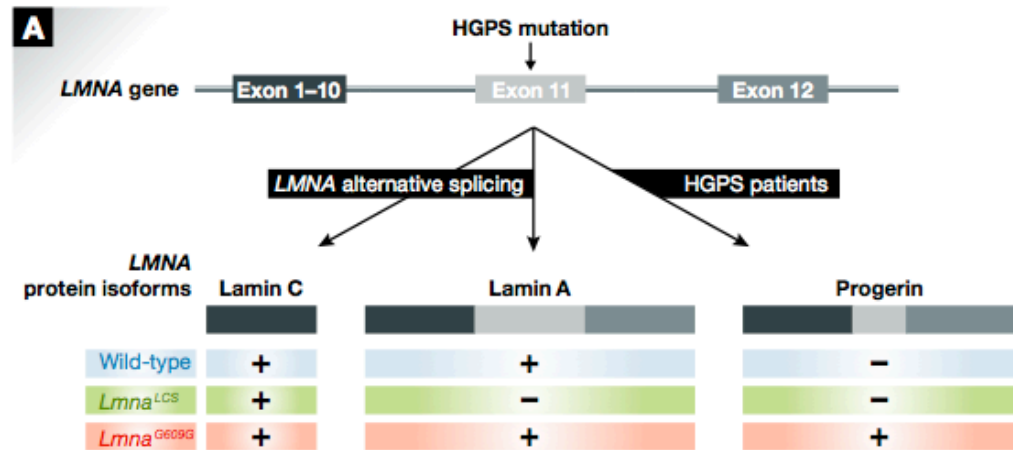
Liver

The two-faced progeria gene and its implications in aging and metabolism

Iliana A Chatzispyrou & Riekelt H Houtkooper

Resveratrol rescues SIRT1–dependent adult stem cell decline and alleviates progeroid features in laminopathy–based progeria

Liu B, Ghosh S, Yang X, Zheng H, Liu X, Wang Z, Jin G, Zheng B, Kennedy BK, Suh Y, Kaeberlein M, Tryggvason K, Zhou Z

Figure 1. SIRT1 Interacts with Lamin A

(A) FLAG-SIRT1 and lamin A were ectopically expressed in HEK293 cells. By western blotting, lamin A was detected in anti-FLAG immunoprecipitates; FLAG-SIRT1 was detected in anti-lamin A/C immunoprecipitates.

(B) In total cell lysates of HEK293 cells, SIRT1 was pulled down by anti-lamin A/C immunoprecipitates and lamin A was pulled down by anti-SIRT1 immunoprecipitates.

(C) Representative immunofluorescence confocal microscopy of SIRT1 and lamin A/C in human fibroblasts. The majority of nuclear SIRT1 colocalizes with lamin A in the nuclear interior (arrows). Scale bar, 5 μm.

(D) Representative confocal microscopy showing colocalization of EGFP-SIRT1 and DsRed-lamin A in human fibroblast cells. Scale bar, 10 μm.

(E) Lamin A but not lamin C was pulled down in anti-FLAG-SIRT1 immunoprecipitates in HEK293 cells.
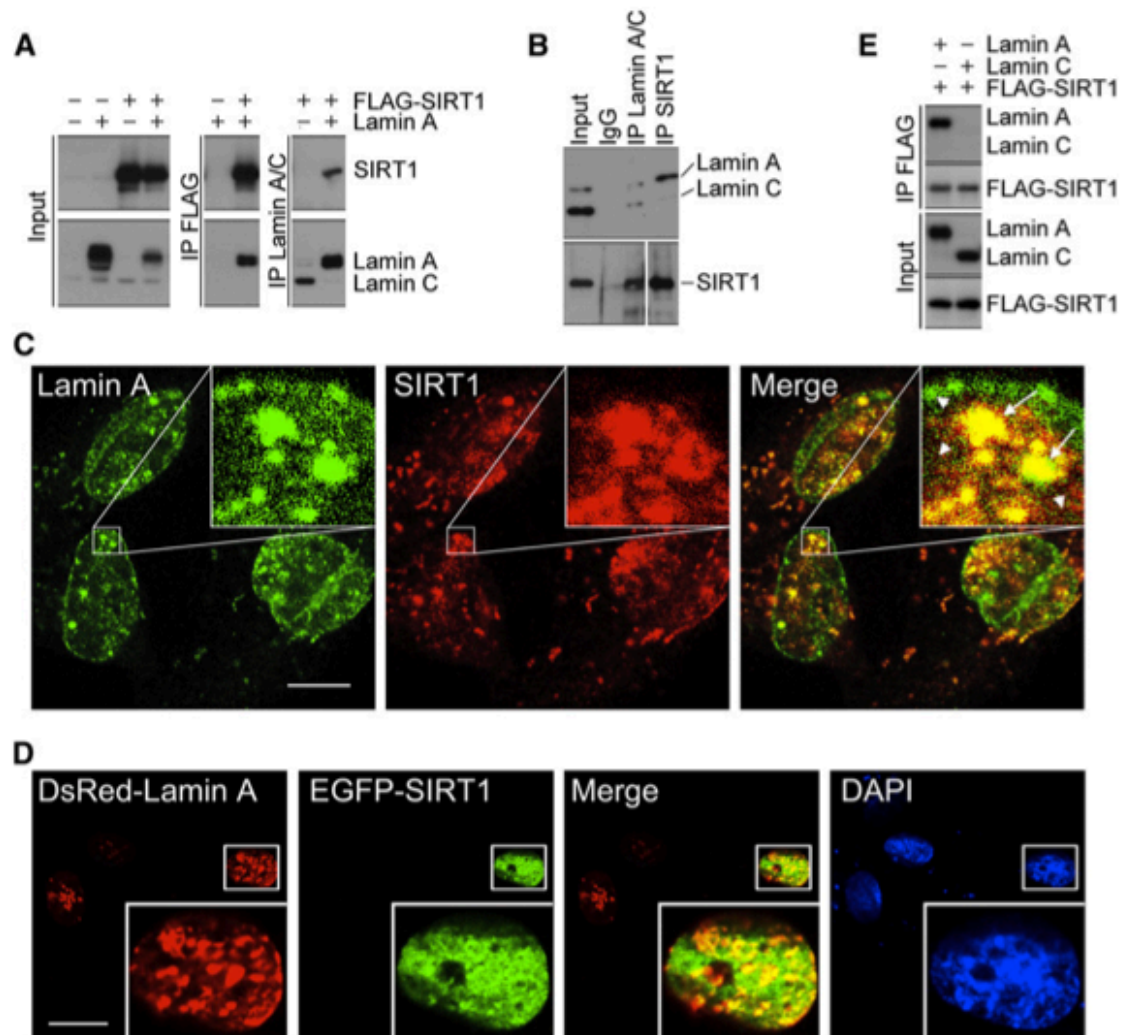
Liu B, Ghosh S, Yang X, Zheng H, Liu X, Wang Z, Jin G, Zheng B,
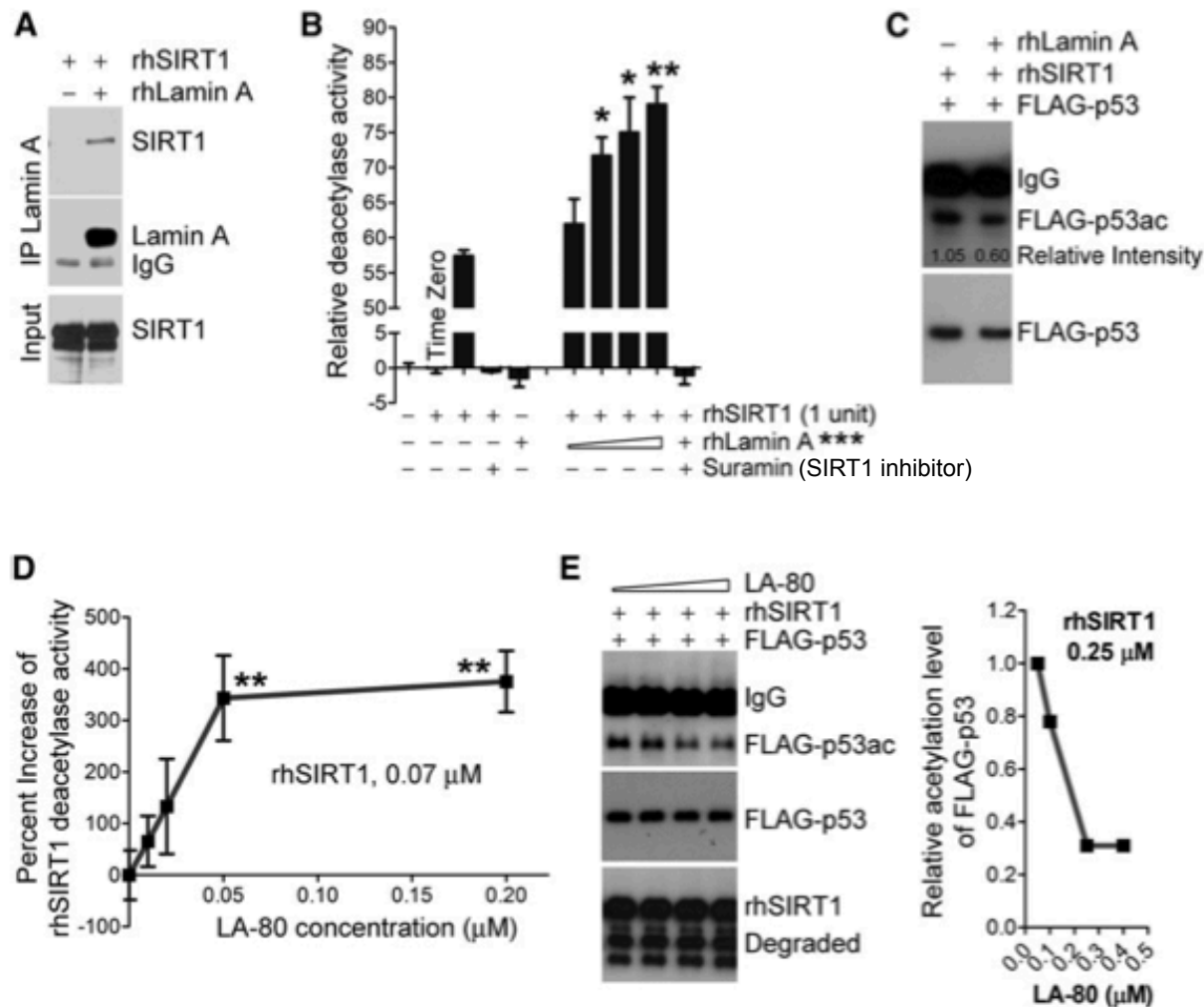Kennedy BK, Suh Y, Kaeberlein M, Tryggvason K, Zhou Z

Figure 2. Lamin A Is an Activator of SIRT1

(A) Recombinant human SIRT1 (rhSIRT1) was pulled down by anti-lamin A immunoprecipitates in test tubes containing rhSIRT1 and recombinant human lamin A (rhLamin A).
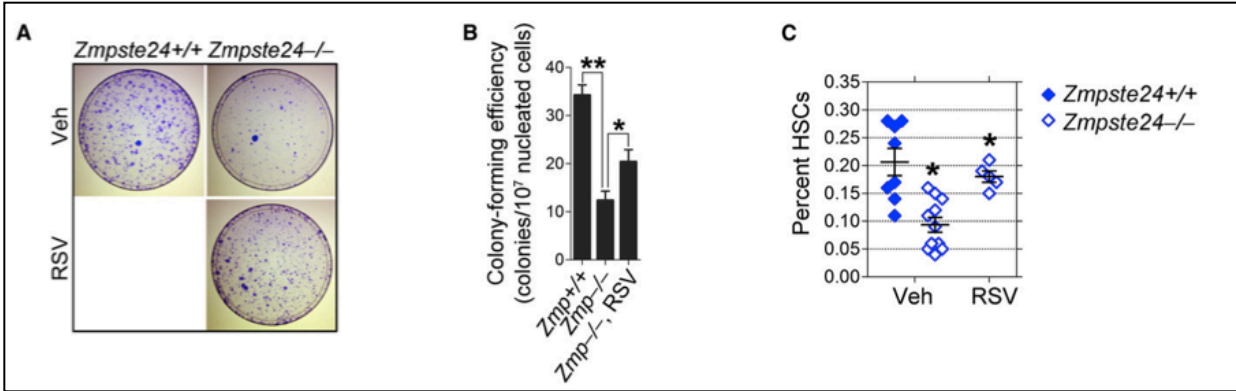
(B) RhSIRT1 deacetylase activity was determined by BioMol SIRT1 Fluorimetric Drug Discovery Kit (BSDK) in the presence or absence of rhLamin A. Data represent mean ± SEM, n = 3. *p < 0.05, **p < 0.01, rhLamin A + rhSIRT1 versus rhSIRT1 only. ***The molar ratios of rhLamin A to rhSIRT1 are 0.5, 1.0, 2.0, and 4.0, respectively.

(C) Acetyl FLAG-p53 was incubated with rhSIRT1 in the presence or absence of rhLamin A. FLAG-p53 acetylation was detected by western blotting with anti-acetyl lysine antibodies. Relative level of acetylated p53 was quantified by ImageJ. *The molar ratio of rhLamin A to rhSIRT1 is 1.

(D) RhSIRT1 deacetylase activity was determined by BioMol SIRT1 Fluorimetric Drug Discovery Kit (BSDK) in the presence or absence of LA-80 (synthetic peptide of carboxyl 80 aa of lamin A). Data represent mean ± SEM, n = 3. **p < 0.01, LA-80 + rhSIRT1 versus rhSIRT1 only.

(E) Acetyl FLAG-p53 was incubated with rhSIRT1 in the presence of various amount of LA-80. FLAG-p53 acetylation was detected by western blotting with anti-acetyl lysine antibodies (left). Relative level of acetylated p53 was quantified by ImageJ (right).

Resveratrol rescues SIRT1–
dependent adult stem cell decline
and alleviates progeroid features in
laminopathy–based progeria

Liu B, Ghosh S, Yang X, Zheng H, Liu X, Wang Z, Jin G, Zheng B,
Kennedy BK, Suh Y, Kaeberlein M, Tryggvason K, Zhou Z

A: Colony formiung capacity BMSC
B: Quantification of A
C: In vivo, animals fed with RSV
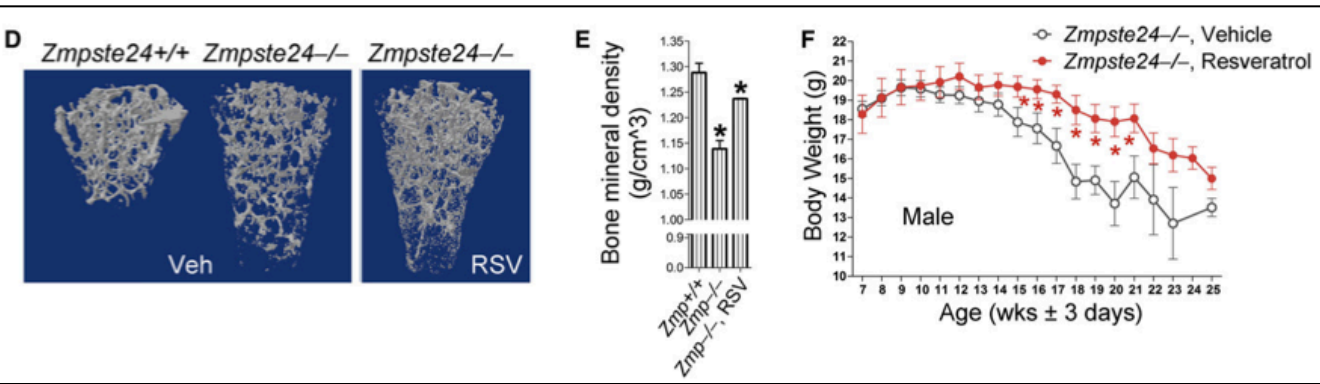
D: Bone trabecular structure

E: Quantification of B

C: Body weight males
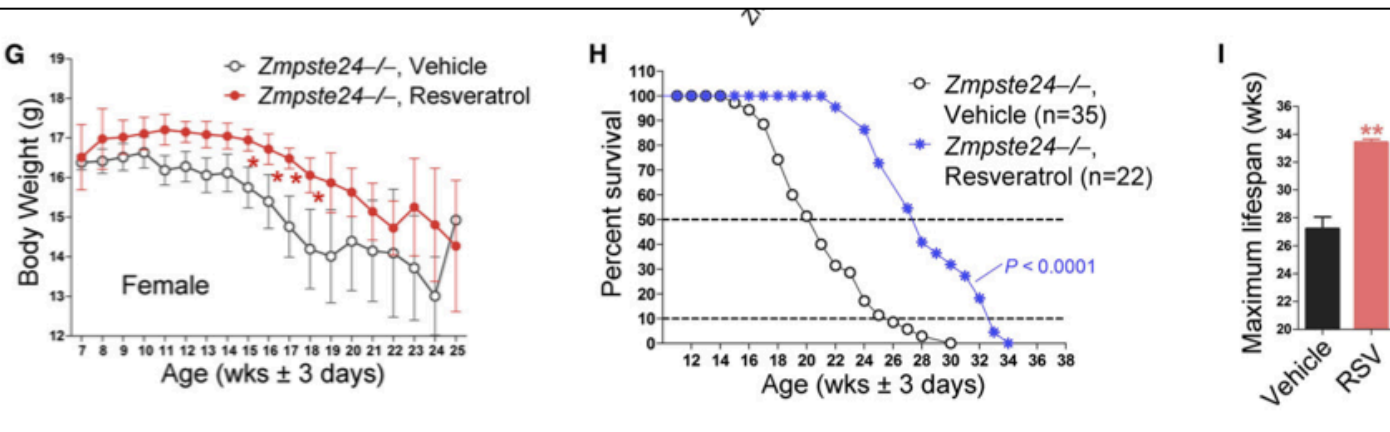
G: Body weight females
H: Lifespan
I: Lifespan